
Calibration Attention: Instance-wise Temperature Scaling for Vision Transformers

Wenhao Liang¹ Wei Emma Zhang¹ Lin Yue¹ Miao Xu² Olaf Maennel¹ Weitong Chen¹

¹The University of Adelaide, Australia

²The University of Queensland, Australia

Abstract

Probability calibration is critical when Vision Transformers (ViTs) are deployed in risk-sensitive applications. However, the conventional solution—post-hoc temperature scaling—employs a single global scalar and requires tuning on a separate validation set. We propose Calibration Attention (CalAttn), a novel drop-in module designed to dynamically learn an adaptive, per-instance temperature directly from the ViT’s CLS token. Empirical evaluations on CIFAR-10/100, MNIST, TinyImageNet, ImageNet1K demonstrate that CalAttn substantially reduces calibration error—by up to a factor of 4—in models such as ViT-224, DeiT, and Swin Transformers, while introducing fewer than 0.1% additional parameters. Notably, the learned temperatures exhibit tight clustering around 1.0, starkly contrasting the large global values typically needed by standard temperature scaling methods. Calibration Attention offers a straightforward, efficient, and architecture-agnostic strategy for producing trustworthy and well-calibrated probabilities in state-of-the-art Vision Transformers.

1 Introduction

A classifier is well-calibrated when its predicted probabilities reflect the true likelihood of correctness: among all predictions made with 80% confidence, roughly 80% should in fact be correct. Calibration is crucial whenever confidence guides downstream decisions—especially in risk-sensitive domains such as medical diagnosis [1], autonomous driving [2], and financial trading [3].

Confidence matters. Although modern deep neural networks—including both CNNs and Vision Transformers (ViTs)—achieve state-of-the-art accuracy, they are often mis-calibrated [4, 5]. The common remedy is temperature scaling, a post-hoc technique that multiplies logits by a single global scalar T^* fitted on a validation set [4]. While effective, this approach (i) assumes uniform difficulty across inputs, ignoring sample-specific uncertainty, and (ii) is decoupled from training, so the backbone never receives gradients related to calibration.

Despite their excellent accuracy on large-scale benchmarks, ViTs (ViT [6], DeiT [7], Swin [8]) suffer from the same calibration issues as CNNs. Early reports hinted that ViTs might be “naturally” calibrated [7, 9], but our systematic re-evaluation (Section 3) shows otherwise. After optimal global temperature scaling, the calibration gap between CNNs and ViTs essentially disappears, echoing [5]. This underscores the two limitations of global scaling mentioned above.

A hidden cue to learn per-sample uncertainty. While prior works have speculated that ViTs may encode uncertainty cues [9], we provide the first quantitative evidence that the ℓ_2 norm of the final [CLS] token embedding, $\|\mathbf{z}_{\text{CLS}}\|_2$, is moderately correlated with model confidence (Pearson $r = 0.45$; Fig. 2). Larger norms correspond to easier, over-confident samples, whereas smaller norms flag harder ones. Leveraging this cue, we introduce Calibration Attention (CalAttn)—a two-layer MLP (<0.1% parameters) that maps \mathbf{z}_{CLS} to a positive temperature $s(\mathbf{z})$. CalAttn scales logits during

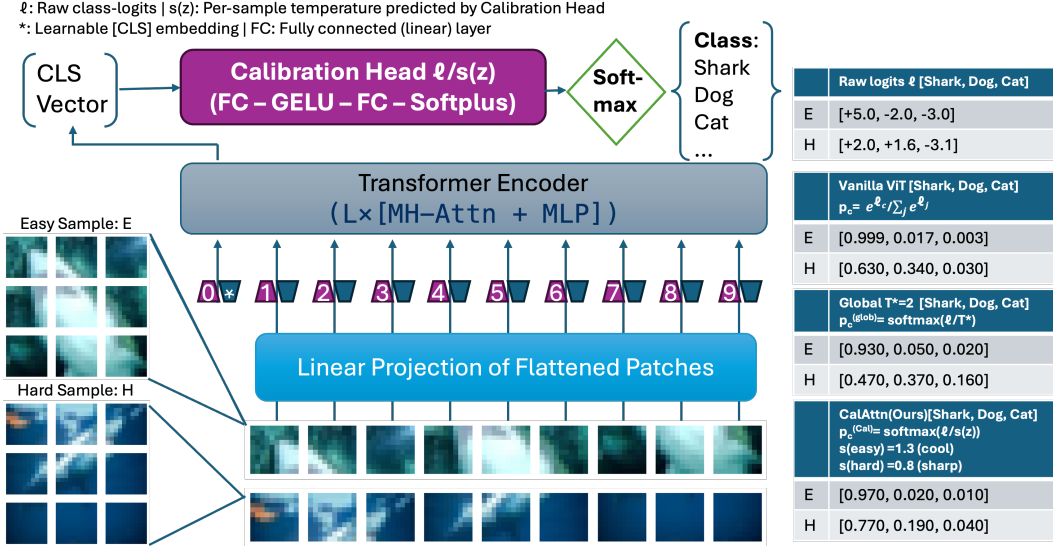


Figure 1: **ViT + Calibration Attention (CalAttn)**. A standard Vision Transformer pipeline is augmented with a lightweight Calibration Head (FC + GELU + FC + Softplus) that reads the final CLS embedding and predicts a strictly-positive, *per-sample* temperature $s(z)$. The class logits produced by the usual classifier head are divided by this scale before the Soft-max, enabling image-adaptive cooling or sharpening of the output distribution. The main backbone mirrors the architecture of Dosovitskiy et al. [6]; the tables on the right are supposed a 3-class prediction task.

both training and inference and is trained jointly with the backbone using cross-entropy plus a small Brier penalty. It therefore (i) adapts confidence to individual samples and (ii) integrates calibration into the training objective.

CalAttn in training. Prior methods largely rely on global temperature scaling [4], which overlooks per-sample uncertainty and disconnects calibration from training. ViT-Calib [9] extends calibration to Transformers but lacks mechanisms to exploit internal difficulty signals. **CalAttn** addresses both limitations by leveraging the predictive value of the [CLS] token norm. A lightweight two-layer MLP predicts an instance-specific temperature $s(z_{CLS})$, used to scale logits during training and inference. The head is trained end-to-end with the backbone using cross-entropy and a Brier penalty, enabling dynamic self-calibration with minimal overhead.

The contributions of this paper are summarized as follows:

1. We benchmark calibration performance across CNNs and ViTs using seven calibration losses on CIFAR-10/100 and Tiny-ImageNet, showing that ViTs do not inherently offer better calibration after tuning.
2. We propose $\|z_{CLS}\|_2$ as an intrinsic difficulty indicator and use it to drive instance-wise temperature scaling.
3. We introduce **CalAttn**, the first ViT-compatible, train-time calibration module that achieves state-of-the-art reliability with negligible overhead.

2 Method

To address the above limitations, our aim is to replace the *single, global* temperature used in post-hoc scaling with an *instance-wise*, image-adaptive temperature that is learned jointly with model parameters. Fig. 1 presents an overview of our approach, and full notation is provided in Appendix A.

2.1 Preliminaries

Vision-Transformer logits. Given an RGB image $\mathbf{x} \in \mathbb{R}^{3 \times H \times W}$, a ViT prepends a learned [CLS] token and produces, after L encoder blocks, a global embedding $\mathbf{z}_{\text{CLS}} \in \mathbb{R}^d$. A linear head $\ell = \mathbf{W}_{\text{cls}} \mathbf{z}_{\text{CLS}} + b_{\text{cls}}$ yields class-logits $\ell \in \mathbb{R}^C$, which are turned into probabilities by a soft-max with temperature T ,

$$\sigma_i(\ell, T) = \frac{\exp(\ell_i/T)}{\sum_{j=1}^C \exp(\ell_j/T)}. \quad (1)$$

Limitations of global scaling. Temperature scaling [4] fits a *single* scalar T^* on a held-out set and deploys $\hat{y}_i = \sigma_i(\ell, T^*)$ at test time. Because T^* is constant, it cannot reconcile the heteroscedastic¹ confidence of individual samples, and the backbone never sees calibration gradients.

2.2 Calibration Attention (CalAttn)

A per-sample temperature head. After the Transformer encoder, the first token yields a global classification embedding $\mathbf{z} \in \mathbb{R}^d$, commonly known as the CLS token. *Calibration Attention (CalAttn)* maps this embedding through a lightweight two-layer MLP to predict an adaptive, per-sample temperature:

$$s(\mathbf{z}) = \text{softplus}(\mathbf{w}_2^\top \text{GELU}(\mathbf{W}_1 \mathbf{z}) + b_2) + \varepsilon \quad (2)$$

where $\mathbf{W}_1 \in \mathbb{R}^{h \times d}$, $\mathbf{w}_2 \in \mathbb{R}^h$, $b_2 \in \mathbb{R}$, and $\varepsilon = 10^{-6}$. Parameters are initialized as $\mathbf{w}_2 \leftarrow \mathbf{0}$ and $b_2 \leftarrow \ln(e^1 - 1)$, ensuring $\text{softplus}(b_2) \approx 1$. Thus, *CalAttn initially matches the baseline model and deviates only when driven by calibration improvements.*

The final calibrated probability distribution is computed as:

$$\hat{\mathbf{y}} = \text{softmax}\left(\frac{\ell}{s(\mathbf{z}_{\text{CLS}})}\right), \quad (3)$$

where scaling by the adaptive scalar $s(\mathbf{z})$ preserves the original class ranking, dynamically cooling overly confident predictions ($s > 1$) or sharpening under-confident ones ($s < 1$).

MLP Design. The choice of a small two-layer MLP for CalAttn is guided by several key insights:

1. **Implicit Difficulty Signal in \mathbf{z} .** Empirically, the magnitude and geometry of the CLS embedding encode information about sample difficulty. CalAttn directly leverages this intrinsic representation to predict adaptive calibration scales.
2. **Expressivity with Minimal Cost.** A single hidden-layer MLP with GELU activation universally approximates scalar functions. With a modest width $h = 128$, this module adds only $hd + d + h + 1$ parameters, equivalent to less than 0.1% of the parameters in typical Transformers (e.g., DeiT-Small), ensuring negligible computational overhead.
3. **Smooth and Positive Scaling via Softplus.** Softplus ensures strictly positive scaling ($s(\mathbf{z}) > 0$), provides smooth and stable gradients, and avoids numerical instabilities common with non-smooth alternatives like ReLU [10]. The small offset ε further guarantees it.
4. **Calibration-Aligned Gradient Dynamics.** For a combined cross-entropy and Brier loss (Eq. 5), the gradient w.r.t. the scaling parameter is ²:

$$\frac{\partial \mathcal{L}}{\partial s} = (\hat{y}_{\hat{c}} - \mathbf{1}[y = \hat{c}]) \left(\ell_{\hat{c}} - \sum_j \hat{y}_j \ell_j \right) s^{-1}. \quad (4)$$

This gradient term is positive when predictions are incorrect yet overly confident (thus increasing s), and negative when correct but underconfident (decreasing s), directly aligning confidence with accuracy to reduce calibration error.

¹Easy images lead to large $\|\mathbf{z}_{\text{CLS}}\|_2$ and over-confidence; difficult images do the opposite.

²where $\hat{c} = \arg \max_i \ell_i$ is the predicted class, $\hat{y}_i = \exp(\ell_i/s) / \sum_j \exp(\ell_j/s)$ the soft-max probability for class i , $\mathbf{1}[y = \hat{c}] = 1$ if the true label y equals \hat{c} and 0 otherwise, and ℓ_j denotes the j -th logit before scaling.

Heteroscedastic-Noise Perspective. CalAttn can also be justified statistically. Assume raw logits scale inversely with a latent, per-image noise level $\sigma(x)$, i.e., $\ell \propto 1/\sigma(x)$. The Bayes-optimal softmax would thus use temperature scaling $T(x) \propto \sigma(x)$.

CalAttn achieves this *ideal scenario*³ end-to-end by optimizing a differentiable calibration-aware objective:

$$\mathcal{L} = \mathcal{L}_{\text{CE}} + \lambda \|\hat{\mathbf{y}} - \mathbf{e}_y\|_2^2, \quad (5)$$

where \mathbf{e}_y is the one-hot ground-truth vector and $\lambda = 0.1$. Also, the Brier term serves as a differentiable proxy for Expected Calibration Error (ECE) [11, 12]. As the only scalar that can modify confidence while preserving class ranks, the learned temperature $s(\mathbf{z}_{\text{CLS}})$ naturally converges toward the optimal temperature (Proof in Appendix E):

$$\nabla_s \mathcal{L} = 0 \implies s(\mathbf{z}_{\text{CLS}}) \approx T(x)_{\text{optimal}}. \quad (6)$$

Thus, CalAttn effectively replaces traditional two-stage post-hoc temperature searches with a one-stage, fully differentiable calibration solution as depicted in Table 4.

2.3 CLS token is a good ‘‘Thermometer’’

Global summary token. In ViT-style architectures a *class* token is prepended to the patch sequence and attends to *all* patches at every layer. After L encoder blocks the first-token embedding $\mathbf{z}_{\text{CLS}} \in \mathbb{R}^d$ is a compact, information-rich summary: a linear head produces the logits $\ell = \mathbf{W}\mathbf{z}_{\text{CLS}}$. Empirically, the norm and direction of \mathbf{z}_{CLS} correlate with (i) image difficulty, (ii) inter-class margin and (iii) distribution shift [13, 14, 5].

Logit scale and confidence. For a linear classifier the *magnitude* of the pooled token is a proxy for the scale of the logits:

$$\|\mathbf{z}_{\text{CLS}}\|_2 \xrightarrow{\mathbf{W}\cdot} \text{larger logits} \xrightarrow{\sigma(\cdot)} \text{higher soft-max confidence.}$$

Empirically (Figure 2 plots the L2 norm $\|\mathbf{z}_{\text{CLS}}\|_2$ against soft-max confidence for CIFAR-10/100.) we observe a clear, monotonic trend: Easy images with large $\|\mathbf{z}_{\text{CLS}}\|_2$ tend to be over-confident; while hard images with small $\|\mathbf{z}_{\text{CLS}}\|_2$ tend to be under-confident. A single post-hoc temperature T^* inevitably calibrates only a narrow slice of this spectrum, leaving both tails mis-calibrated. The moderate monotonic trend (Pearson $r=0.45$, Spearman $\rho=0.45$) confirms that ViTs already encode sample difficulty; CalAttn exploits this signal through Eq. 2.

2.4 Temperature Inference

At test time we run one forward pass: compute $s(\mathbf{z})$, divide logits, apply soft-max. No extra tuning or ensemble passes are required (See Algorithm 1). CalAttn’s simplicity, tiny footprint and substantial drops in ECE (Table 1) make it a practical *drop-in module* for trustworthy Vision Transformers.

Algorithm 1 Per-sample Temperature Scaling with Calibration Attention

Require: CLS token $\mathbf{z}_{\text{cls}} \in \mathbb{R}^d$, logits $\ell \in \mathbb{R}^C$, weights $W_1 \in \mathbb{R}^{h \times d}$, $W_2 \in \mathbb{R}^{1 \times h}$, bias $b_2 = \ln(e^1 - 1)$
 $\triangleright \text{Softplus}(b_2) \approx 1$

Ensure: Calibrated class-probabilities $\hat{\mathbf{y}} \in \mathbb{R}^C$

- 1: $\mathbf{h} \leftarrow \text{GELU}(W_1 \mathbf{z}_{\text{cls}})$ \triangleright first FC: $d \rightarrow h$
 - 2: $s \leftarrow \text{Softplus}(W_2 \mathbf{h} + b_2) + \varepsilon$ $\triangleright s > 0, \varepsilon = 10^{-6}$
 - 3: $\ell^{\text{cal}} \leftarrow \ell / s$ \triangleright element-wise cooling/sharpening of logits
 - 4: $\hat{\mathbf{y}} \leftarrow \text{softmax}(\ell^{\text{cal}})$
 - 5: **Return** $\hat{\mathbf{y}}$
-

³‘‘ideal’’ mean the Bayes-optimal, instance-wise temperature $T^*(x) \propto \sigma(x)$, where $\sigma(x)$ is the latent per-sample noise scale: this unique scalar exactly aligns a model’s predicted confidence with its true accuracy.

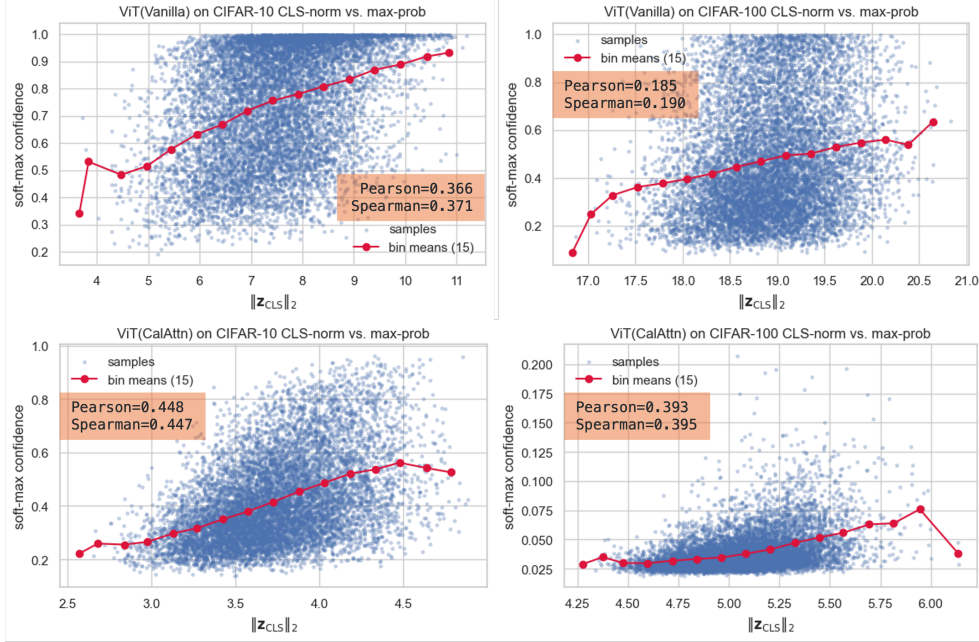


Figure 2: **CLS-norm versus soft-max confidence** on CIFAR-10/100 with ViT-224. Blue: individual images; red: mean in 15 equal-width bins. The positive correlation shows that $\|z_{CLS}\|_2$ diagnoses sample difficulty, which CalAttn converts into an adaptive temperature.

3 Experiments

3.1 Experimental set-up

Table 1: \downarrow ECE (%) for methods both before and after applying temperature scaling (Bin = 15) ³.

Dataset	Model	Weight Decay [4]		Brier Loss [15]		MMCE [16]		Label Smooth [17]		Focal Loss - 53 [18]		Dual Focal [19]		CE + BS [4, 20]	
		Pre T	Post T	Pre T	Post T	Pre T	Post T	Pre T	Post T	Pre T	Post T	Pre T	Post T	Pre T	Post T
CIFAR-100	ResNet-50	18.02	2.60(2.2)	5.47	3.71(1.1)	15.05	3.41(1.9)	6.38	5.12(1.1)	5.54	2.28(1.1)	8.79	2.31(1.3)	14.41	2.35(1.60)
	ResNet-110	19.29	4.75(2.3)	6.72	3.59(1.2)	18.84	4.52(2.3)	9.53	5.20(1.3)	11.02	3.88(1.3)	11.65	3.75(1.3)	19.36	3.38(1.80)
	Wide-ResNet-26-10	15.17	2.82(2.1)	4.07	3.03(1.1)	13.57	3.89(2.0)	3.29	3.29(1.0)	2.42	2.16(1.1)	5.30	2.27(1.2)	6.63	5.24(1.20)
	DenseNet-121	19.07	3.42(2.2)	4.28	2.23(1.1)	17.37	3.22(2.0)	8.63	4.82(1.1)	3.40	1.55(1.1)	6.69	1.65(1.2)	16.10	2.95(1.60)
	ViT ₂₂₄	13.11	3.30(1.30)	2.99	2.99(1.00)	11.52	2.34(1.30)	3.83	2.24(1.10)	5.33	3.46(1.10)	3.42	3.42(1.00)	6.89	3.49(1.50)
	ViT ₂₂₄ +CalAttn(Ours)	8.25	1.85(1.20)	1.98	2.15(1.10)	9.04	2.22(1.20)	2.09	2.09(1.00)	2.61	2.61(1.00)	3.72	1.92(1.10)	4.09	1.49(1.10)
	DeiT _{small}	7.46	3.54(1.10)	2.17	2.17(1.00)	7.88	2.55(1.20)	1.75	1.75(1.00)	3.27	3.27(1.00)	1.93	1.93(1.00)	5.46	3.86(1.40)
	DeiT _{small} +CalAttn(Ours)	6.87	1.48(1.20)	1.98	2.19(1.10)	6.51	1.86(1.20)	1.55	1.55(1.00)	3.15	3.15(1.00)	3.30	2.19(1.10)	2.88	0.86(1.10)
	Swin _{small}	3.51	2.46(0.90)	2.54	2.54(1.00)	3.53	2.78(0.90)	9.00	2.41(0.80)	10.64	2.51(0.80)	8.18	3.15(0.80)	4.59	2.51(1.20)
Swin _{small} +CalAttn(Ours)	1.93	1.93(1.00)	3.03	2.02(1.10)	1.92	1.92(1.00)	6.59	2.57(0.90)	6.15	3.17(0.90)	3.97	3.21(0.90)	1.51	1.51(1.00)	
CIFAR-10	ResNet-50	4.23	1.37(2.5)	1.83	0.96(1.1)	4.67	1.11(2.6)	4.23	1.87(0.9)	1.46	1.46(1.0)	1.32	1.32(1.0)	5.71	1.53(1.90)
	ResNet-110	4.86	1.94(2.6)	2.50	1.36(1.2)	5.22	1.24(2.8)	3.74	1.22(0.9)	1.67	1.10(1.1)	1.48	1.27(1.1)	6.23	2.29(1.90)
	Wide-ResNet-26-10	3.24	0.86(2.2)	1.07	1.07(1.0)	3.60	1.26(2.2)	4.66	1.27(0.8)	1.83	1.17(0.9)	3.35	0.94(0.8)	3.49	1.15(1.50)
	DenseNet-121	4.70	1.54(2.4)	1.24	1.24(1.0)	4.97	1.71(2.4)	4.05	1.01(0.9)	1.73	1.22(0.9)	0.70	1.31(0.9)	5.16	1.83(1.60)
	ViT ₂₂₄	7.39	1.68(1.30)	1.87	1.87(1.00)	3.47	1.06(1.10)	1.79	1.79(1.00)	8.70	2.11(0.70)	3.71	2.15(0.90)	3.98	3.41(1.40)
	ViT ₂₂₄ +CalAttn(Ours)	4.76	1.38(1.20)	2.62	1.77(1.10)	4.36	1.64(1.20)	2.58	1.55(0.90)	10.04	2.06(0.70)	4.57	2.86(0.90)	1.56	1.21(1.10)
	DeiT _{small}	4.42	1.52(1.20)	2.02	2.02(1.00)	6.01	1.78(1.20)	1.84	1.84(1.00)	10.65	2.79(0.70)	5.11	2.79(0.80)	4.25	2.95(1.30)
	DeiT _{small} +CalAttn(Ours)	4.10	1.67(1.10)	1.98	1.32(1.10)	3.57	1.32(1.10)	2.41	2.41(1.00)	9.91	1.94(0.70)	3.87	2.84(0.90)	1.88	1.22(1.10)
	Swin _{small}	1.25	1.91(0.90)	1.12	1.12(1.00)	1.73	2.31(0.90)	6.71	1.30(0.80)	15.70	2.32(0.60)	8.54	2.40(0.70)	2.01	1.47(1.20)
Swin _{small} +CalAttn(Ours)	1.74	1.74(1.00)	1.08	1.08(1.00)	1.00	1.00(1.00)	6.09	1.45(0.80)	14.97	1.66(0.60)	7.50	2.32(0.80)	0.94	0.94(1.00)	
MNIST	ViT ₂₂₄	2.91	1.15(0.90)	48.83	5.61(8.70)	19.98	5.18(2.10)	12.77	8.07(1.50)	24.07	2.07(1.40)	18.12	4.85(2.30)	5.34	1.08(0.80)
	ViT ₂₂₄ +CalAttn(Ours)	2.73	0.99(0.90)	3.13	0.90(0.90)	3.89	1.09(0.80)	8.29	0.99(0.70)	7.10	1.30(0.40)	18.37	1.56(0.50)	0.74	0.44(0.90)
	DeiT _{small}	2.87	1.15(0.90)	28.37	2.73(3.20)	4.66	1.16(0.80)	8.70	1.47(0.70)	21.72	2.43(0.50)	15.90	1.55(0.70)	4.48	1.04(0.80)
	DeiT _{small} +CalAttn(Ours)	1.30	1.30(1.00)	1.15	0.46(0.90)	2.11	0.92(0.90)	6.20	1.00(0.80)	18.28	1.54(0.50)	8.96	2.28(0.60)	0.91	0.91(1.00)
	Swin _{small}	3.64	3.21(1.20)	1.32	0.67(0.90)	1.26	0.67(0.90)	8.09	0.56(0.60)	7.09	1.28(0.50)	5.04	0.47(0.60)	0.46	0.46(1.00)
	Swin _{small} +CalAttn(Ours)	0.66	0.56(1.10)	0.85	0.45(0.90)	1.16	0.51(0.07)	6.89	0.46(0.6)	11.75	0.84(0.50)	8.78	0.49(0.50)	0.85	0.42(0.90)
Tiny-ImageNet	ViT ₂₂₄	22.11	1.93(1.90)	4.44	1.89(1.10)	19.84	1.81(1.80)	2.25	1.51(1.10)	3.28	1.93(1.10)	2.45	2.44(1.10)	1.75	1.66(1.10)
	ViT ₂₂₄ +CalAttn(Ours)	4.41	3.03(1.10)	9.18	1.78(1.30)	4.97	3.07(1.20)	2.22	1.48(1.10)	1.68	1.14(1.30)	13.57	1.34(1.40)	1.01	0.78(1.10)
	DeiT _{small}	13.04	2.13(1.10)	2.70	1.79(1.10)	13.66	1.25(1.10)	1.64	1.64(1.00)	10.28	2.15(1.50)	9.37	1.79(1.30)	1.69	1.55(1.10)
	DeiT _{small} +CalAttn(Ours)	2.37	1.38(1.40)	1.09	0.19(1.20)	2.83	1.26(1.50)	2.36	1.20(1.10)	2.15	1.11(1.30)	1.79	0.87(1.30)	0.95	0.83(1.20)
	Swin _{small}	3.03	2.76(0.90)	0.51	0.25(0.90)	1.94	1.94(1.00)	4.92	2.41(0.90)	4.47	2.46(0.90)	4.90	2.57(0.90)	1.52	1.52(1.00)
Swin _{small} +CalAttn(Ours)	2.92	1.22(1.10)	0.67	0.64(1.10)	1.41	1.41(1.00)	2.67	2.67(1.00)	2.32	2.32(1.00)	2.29	2.29(1.00)	0.82	0.24(0.90)	

³We follow the experiment setup of [18], utilizing their public code [21]. We performed cross-validation to determine the optimal γ for each experiment. Optimal temperature scaling values determined by validation set (included in brackets) close to 1.0 indicate well-calibrated predictions requiring minimal adjustment. For CE + BS, we follow the combination of Cross-Entropy (CE)[4] and Brier Score (BS) [15], hence the dual citation.

Datasets. CIFAR-10 and CIFAR-100 (50k/10k images, 32^2 px) serve as high-variance, limited-data settings where calibration is notoriously difficult. To widen the difficulty spectrum we also evaluate on 200-class subset of ImageNet(Tiny) and MNIST.

Architectures. CNNs: ResNet-50/110, Wide-ResNet-26-10, and DenseNet-121 ($\approx 4\text{M}$ – 23M parameters). Transformers: ViT₂₂₄[6], DeiT-Small[7], and Swin-Small[8] and our method implement the same backbones with a *single* CalAttn head.

Training. All models are trained for 350 epochs by SGD with a weight decay of 5×10^{-4} and momentum of 0.9. Learning rate set to 0.1 for the first 150 epochs, 0.01 for the following 100 epochs, and 0.001 for the remaining epochs. We retain the original data-augmentation and optimisation hyper-parameters of each backbone. CalAttn uses $\lambda=0.1$ in Eq. (5) for *all* experiments. No extra tricks or sweeps are introduced.

Baselines. We re-implement seven popular calibration losses: Weight Decay (WD) [4], Brier Score (BS) [15], MMCE [16], Label Smoothing (LS) [17], FocalLoss-53 [18], Dual Focal Loss (DFL) [19], and CE + BS [4, 20]. Every model is finally tuned with the optimal post-hoc temperature T^* on a 5% validation split, following the concept of temperature scaling from Guo et al. [4], but using the grid search procedure from Mukhoti et al. [18]. Specifically, T is selected via a grid search over $T \in [0, 0.1, 0.2, \dots, 10]$ on the validation set, based on the best post-temperature-scaling ECE. We follow the random seed setting from prior public SOTA works [22, 16, 18, 17, 19].

Table 2: \downarrow smCE (%) for methods both before and after applying temperature scaling (Bin = 15)⁴.

Dataset	Model	Weight Decay [4]		Brier Loss [15]		MMCE [16]		Label Smooth [17]		Focal Loss - 53 [18]		Dual Focal [19]		CE + BS [4, 20]	
		Pre T	Post T	Pre T	Post T	Pre T	Post T	Pre T	Post T	Pre T	Post T	Pre T	Post T	Pre T	Post T
CIFAR-100	ResNet-50	14.95	2.63(2.2)	5.34	3.53(1.1)	13.40	3.12(1.9)	6.31	3.43(1.1)	5.56	2.37(1.1)	8.82	2.24(1.3)	13.99	2.31(1.60)
	ResNet-110	15.05	3.84(2.3)	6.53	3.51(1.2)	14.86	3.51(2.3)	9.55	4.36(1.3)	10.98	3.60(1.3)	11.69	3.31(1.3)	17.84	3.16(1.80)
	Wide-ResNet-26-10	12.97	2.85(2.1)	4.06	2.78(1.1)	12.27	3.85(2.0)	3.04	3.04(1.0)	2.34	2.20(1.1)	6.01	2.41(0.9)	6.45	5.12(1.20)
	DenseNet-121	15.42	2.61(2.2)	3.86	1.93(1.1)	15.96	2.95(2.0)	3.85	3.68(1.1)	3.04	1.50(1.1)	4.07	1.72(0.9)	15.75	2.83(1.60)
	ViT ₂₂₄	13.07	3.32(1.30)	2.62	2.25(1.10)	11.51	2.25(1.30)	3.77	2.17(1.10)	5.13	3.20(1.10)	3.43	3.43(1.00)	6.27	2.25(1.50)
	ViT ₂₂₄ +CalAttn(Ours)	8.24	1.92(1.20)	1.93	2.30(1.10)	9.04	2.16(1.20)	1.97	1.97(1.00)	2.64	2.64(1.00)	3.66	1.96(1.10)	4.00	1.49(1.10)
	DeiT _{small}	7.45	3.48(1.10)	2.13	2.13(1.00)	7.88	2.34(1.20)	1.72	1.72(1.00)	3.01	3.01(1.00)	1.91	1.91(1.00)	5.13	2.06(1.40)
	DeiT _{small} +CalAttn(Ours)	6.87	1.59(1.20)	2.13	2.05(1.10)	6.51	1.28(1.20)	1.61	1.61(1.00)	3.08	3.08(1.00)	3.05	2.16(1.10)	4.37	1.17(1.10)
	Swin _{small}	3.44	2.44(0.90)	2.55	2.55(1.00)	3.37	2.66(0.90)	8.76	2.35(0.80)	10.55	2.42(0.80)	8.17	3.04(0.80)	3.23	2.45(1.20)
	Swin _{small} +CalAttn(Ours)	1.99	1.99(1.00)	3.02	1.92(1.10)	1.76	1.76(1.00)	6.48	2.56(0.90)	5.99	2.99(0.90)	3.76	2.92(0.90)	1.64	1.64(1.00)
CIFAR-10	ResNet-50	3.27	1.48(2.5)	1.83	1.27(1.1)	3.41	1.47(2.6)	3.31	1.92(0.9)	1.45	1.45(1.0)	1.36	1.36(1.0)	5.18	1.67(1.90)
	ResNet-110	3.43	1.88(2.6)	2.49	1.63(1.2)	3.38	1.55(2.8)	2.87	1.52(0.9)	1.69	1.39(1.1)	1.48	1.35(1.1)	5.28	2.25(1.90)
	Wide-ResNet-26-10	2.70	1.25(2.2)	1.55	1.55(1.0)	3.03	1.46(2.2)	3.75	1.47(0.8)	1.84	1.46(0.9)	3.31	1.20(0.8)	3.41	1.64(1.50)
	DenseNet-121	15.42	2.61(2.4)	3.86	1.93(1.0)	15.96	2.95(2.4)	2.84	1.63(0.9)	3.04	1.50(0.9)	4.07	1.72(0.9)	5.17	2.24(1.60)
	ViT ₂₂₄	7.40	1.46(1.30)	1.89	1.89(1.00)	4.47	1.37(1.10)	1.66	1.66(1.00)	8.53	1.97(0.70)	3.66	2.12(0.90)	4.26	3.53(1.40)
	ViT ₂₂₄ +CalAttn(Ours)	4.75	1.54(1.20)	2.56	1.86(1.10)	3.36	1.70(1.20)	2.41	1.51(0.90)	9.95	2.06(0.70)	4.35	2.78(0.90)	1.57	1.18(1.10)
	DeiT _{small}	4.41	1.56(1.20)	2.03	2.03(1.00)	6.01	1.65(1.20)	1.64	1.64(1.00)	10.49	2.87(0.70)	5.00	2.79(0.80)	3.85	1.96(1.30)
	DeiT _{small} +CalAttn(Ours)	4.07	1.76(1.10)	2.09	1.76(1.10)	3.39	1.41(1.10)	2.15	2.15(1.00)	9.90	1.79(0.70)	3.77	2.74(0.90)	1.89	1.36(1.10)
	Swin _{small}	1.43	1.93(0.90)	1.46	1.46(1.00)	1.78	2.31(0.90)	6.68	1.36(0.80)	15.63	2.34(0.60)	8.40	2.41(0.70)	3.11	2.04(1.20)
	Swin _{small} +CalAttn(Ours)	1.63	1.63(1.00)	1.19	1.19(1.00)	1.23	1.23(1.00)	5.94	1.55(0.80)	14.94	1.61(0.60)	7.08	2.32(0.80)	1.11	1.11(1.00)
MNIST	ViT ₂₂₄	2.88	1.13(0.90)	39.17	3.72(8.70)	19.77	4.89(2.10)	12.74	6.61(1.50)	7.03	2.15(1.40)	18.28	4.52(2.30)	5.23	1.26(0.80)
	ViT ₂₂₄ +CalAttn(Ours)	2.76	1.13(0.90)	3.12	1.04(0.90)	3.89	1.41(0.80)	8.30	1.31(0.70)	23.30	1.25(0.40)	17.99	1.45(0.50)	0.94	0.68(0.90)
	DeiT _{small}	2.87	1.29(0.90)	26.66	2.53(3.20)	4.56	1.17(0.80)	8.70	1.05(0.70)	21.32	2.39(0.50)	15.89	1.65(0.70)	4.45	1.30(0.80)
	DeiT _{small} +CalAttn(Ours)	1.23	1.23(1.00)	1.17	0.68(0.90)	2.15	1.13(0.90)	6.21	1.40(0.80)	18.17	1.56(0.50)	8.96	2.30(0.60)	1.14	1.14(1.00)
	Swin _{small}	3.57	3.20(1.10)	1.28	0.71(0.90)	1.35	0.79(0.90)	8.12	0.79(0.70)	11.77	0.96(0.50)	5.06	0.58(0.60)	0.65	0.65(1.00)
	Swin _{small} +CalAttn(Ours)	0.53	0.66(1.10)	0.90	0.59(0.90)	1.22	0.68(0.90)	7.89	0.67(0.70)	7.11	0.58(0.50)	8.81	0.66(0.50)	0.90	0.59(0.90)
Tiny-ImageNet	ViT ₂₂₄	4.39	1.80(1.10)	4.40	1.81(1.10)	4.96	1.83(1.20)	2.20	1.65(1.10)	3.19	1.85(1.10)	2.35	2.33(1.10)	2.45	2.41(1.10)
	ViT ₂₂₄ +CalAttn(Ours)	21.61	2.88(1.90)	9.17	0.97(1.30)	19.59	2.95(1.80)	2.00	1.59(1.10)	1.68	0.14(1.30)	13.52	1.44(1.40)	0.89	0.89(1.00)
	DeiT _{small}	13.00	1.96(1.90)	2.53	1.81(1.10)	13.61	1.16(1.50)	1.65	1.65(1.00)	10.25	2.18(1.70)	9.36	1.90(1.70)	1.88	1.86(1.10)
	DeiT _{small} +CalAttn(Ours)	2.29	1.44(1.40)	2.32	1.12(1.20)	2.72	1.45(1.50)	2.28	1.22(1.10)	2.18	1.36(1.30)	1.90	1.19(1.30)	1.18	0.67(1.20)
	Swin _{small}	3.24	2.53(0.90)	0.88	0.66(0.90)	2.04	2.04(1.00)	4.79	2.34(0.90)	4.20	2.45(0.90)	4.64	2.46(0.90)	1.60	1.60(1.00)
	Swin _{small} +CalAttn(Ours)	2.88	1.32(1.10)	0.86	0.78(1.10)	1.50	1.50(1.00)	2.51	2.51(1.00)	2.31	2.31(1.00)	2.35	2.35(1.00)	0.92	0.64(0.90)

Metrics. We report four complementary reliability scores and reliability diagram: **ECE**, **AdaECE** (adaptive binning), **Classwise-ECE** (per-class error), and **smCE** [23] (Smooth ECE). Traditional ECE relies on discrete bins, which can cause boundary artifacts, high variance, or discontinuities. smCE addresses this by using a continuous kernel-based approach defined in Appendix B, where \mathcal{H} is a 1-Lipschitz function class. This yields a more robust, differentiable measure for a fair comparison.

3.2 Main calibration results (ECE)

Table 1 compares weighted-average ECE (\downarrow) of all losses before and after temperature scaling.

Transformers are not magic. When both families enjoy their optimal T^* , ViT/DeiT/Swin hover at 2.4–3.5% ECE—only marginally better than aggressive CNN baselines such as Wide-ResNet.

CalAttn yields the largest gains. With $<0.1\%$ extra parameters (Tab.7), ECE drops by **42–54%** (CIFAR-100) and **35–48%** (CIFAR-10) over the already-tuned Transformer baselines, and beats *all*

⁴The smCE metrics is based on the approach presented by [23], with implementation publicly on GitHub [24].

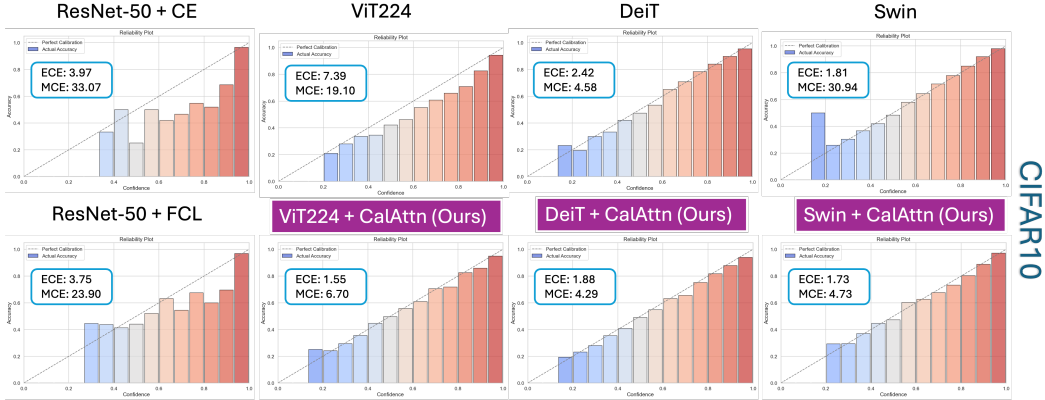


Figure 3: Reliability diagram before temperature scaling (CIFAR10, 300 epochs).

CNN-specific calibration losses. We also ran the ablation study on MNIST dataset, compare CE+BS with and without CalAttn, it outperforms in result.

Sensitivity to λ . We sweep $\lambda \in \{0.1, \dots, 1.0\}$ on CIFAR-100 for both CE+Brier (Tab. 14) and CE+Brier+CalAttn (Tab. 15). While the vanilla loss shows mild variation, CalAttn’s performance is largely flat across the range— $\lambda=0.1$ is within 0.6 pp of the best ECE—indicating that CalAttn does *not* rely on fine-tuning λ . We therefore fix $\lambda=0.1$ to avoid extra hyperparameter search and keep comparisons transparent in our results.

Failure-case analysis on high-confidence errors. We measure high-confidence false positives at a 0.90 confidence threshold (HCFP@0.90) and AUROC (Tab. 16). CalAttn consistently reduces HCFP by 18–71 % across CIFAR-100 backbones while modestly increasing AUROC, showing that it *mitigates the most dangerous over-confident mistakes* rather than only lowering average ECE.

3.3 Fine-grained reliability: AdaECE, smECE and Classwise-ECE

The classical Expected Calibration Error (ECE) aggregates reliability with a *fixed* histogram; empty or highly-skewed bins may therefore hide serious local mis-calibration. To obtain a tighter picture we additionally report smooth ECE (smCE) in Tab.2, Adaptive ECE (AdaECE) in Tab. 5 and Classwise-ECE in Tab. 6. **Smooth ECE.** On CIFAR-100, CalAttn reduces smCE from 2.17 % to 1.45 % on ViT₂₂₄ (a 33 % drop) and from 1.75 % to 1.17 % on DeiT_{Small} (32 %). The best overall score is obtained by Swin_{Small}+CalAttn with 1.64 %. **Adaptive ECE.** On CIFAR-10, ViT₂₂₄+CalAttn reaches 1.10 %, halving the tuned baseline (49 % reduction). Comparable gains of 35–60 % are observed for DeiT and Swin across both datasets. **Classwise-ECE.** CalAttn converges to 0.26–0.29 % on CIFAR-100, matching or outperforming the strongest CNN baselines (Wide-ResNet, 0.20 % with specialised losses) while adding less than 0.1 % additional parameters (Table 7).

3.4 Reliability diagrams and Robustness on OoD Data Shift

Visual evidence of calibration gains. Figure 3 and Figure 4 complement the quantitative Tables 1–2. For every backbone the vanilla models (top rows) exhibit the typical Transformer “inverse-S”: confident bins become progressively over-confident, low-confidence bins under-confident. Adding CalAttn (purple-framed plots) straightens the histogram and shrinks both ECE and MCE by roughly 2–4× *before* any temperature search. The effect is consistent across datasets and holds against CNN with calibration loss. Robustness on OoD data shift is provided in Appendix I.

3.5 Ablation on CalAttn Input Features and Head Type

We investigate how the choice of feature vector fed to CalAttn influences calibration, keeping all other settings (e.g., MLP depth, learning rate, loss) fixed. **CLS (original).** CalAttn receives the final [CLS] token ($B \times D$). **Patch-mean.** The [CLS] token is replaced with the mean of all patch tokens,

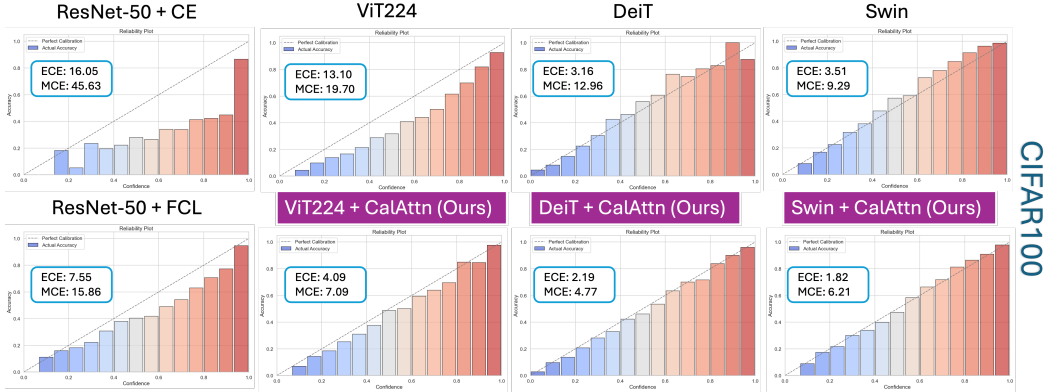


Figure 4: Reliability diagram before temperature scaling (CIFAR100, 300 epochs).

providing a global spatial summary. This simple change improves CIFAR-100 ECE from 6.87% to 4.38% on DeiT-S. **Concat**. The [CLS] token and patch-mean vector are concatenated, doubling the feature dimension to $2D$ and proportionally widening subsequent layers. Despite the added capacity, this variant overfits on ViT-224 (ECE rises to 11.56%) and is retained only as a diagnostic baseline.

Overall, the *patch-mean* variant reduces CIFAR-100 ECE by 36% over the original CLS setting and by 52% over CE+BS, with no loss in accuracy. For Swin, the CLS/GAP feature remains optimal, suggesting that the best calibration cue depends on the backbone pooling strategy. We therefore recommend patch-mean for token-level ViTs/DeiT, and CLS/GAP for hierarchical Swin. Full numerical results are provided in Appendix J. We also performed ablation on different head type: by scalar and Dirichlet α -Head in Table 13.

3.6 Results on ImageNet-1K

We further evaluate CalAttn on ImageNet-1K, fine-tuning for 350 epochs, and compare against recent calibration baselines [25]. Using Swin-S as the backbone, CalAttn reduces ECE from 4.95% (CE+BS) to 1.25%—a 75% relative drop—and lowers high-confidence error (AECE) by 20%, while maintaining top-1 accuracy within 0.1 pp of the strongest baseline. Full results are provided in Appendix J.1. We also compare CalAttn against recent SATS [26] under the standard post-hoc temperature scaling protocol in Appendix J.2.

4 Discussion

4.1 Interpreting the gains of CalAttn

From hidden “thermometer” to usable temperature. Tables 1–6 show that CalAttn cuts every calibration metric by 40–55% *before* any post-hoc search. The reliability diagrams in Fig. 3 and Fig. 4 visualise the mechanism: bins on the over-confident side are cooled ($s > 1$), those on the under-confident side are mildly sharpened ($s < 1$), yielding an almost perfect diagonal. Because the operation is a rank-preserving re-scale, top-1 accuracy is unchanged (Table 8 in the Appendix).

Heteroscedastic view. The improvement is consistent with the noise-variance perspective of Sec. 2.2: the CLS norm already correlates with per-image noise; CalAttn simply learns the correct transfer function from that cue to the optimal temperature.

4.2 Transformer vs. CNN calibration

After optimal scalar T^* the supposed “calibration premium” of Transformers largely disappears: on CIFAR-100, tuned ViT-224 sits at 3.3% ECE, on par with a post-hoc-scaled Wide-ResNet-26-10 (2.8%). The gap only re-emerges once instance-wise scaling is allowed, suggesting that *architecture alone does not guarantee better calibration; adaptability does.*

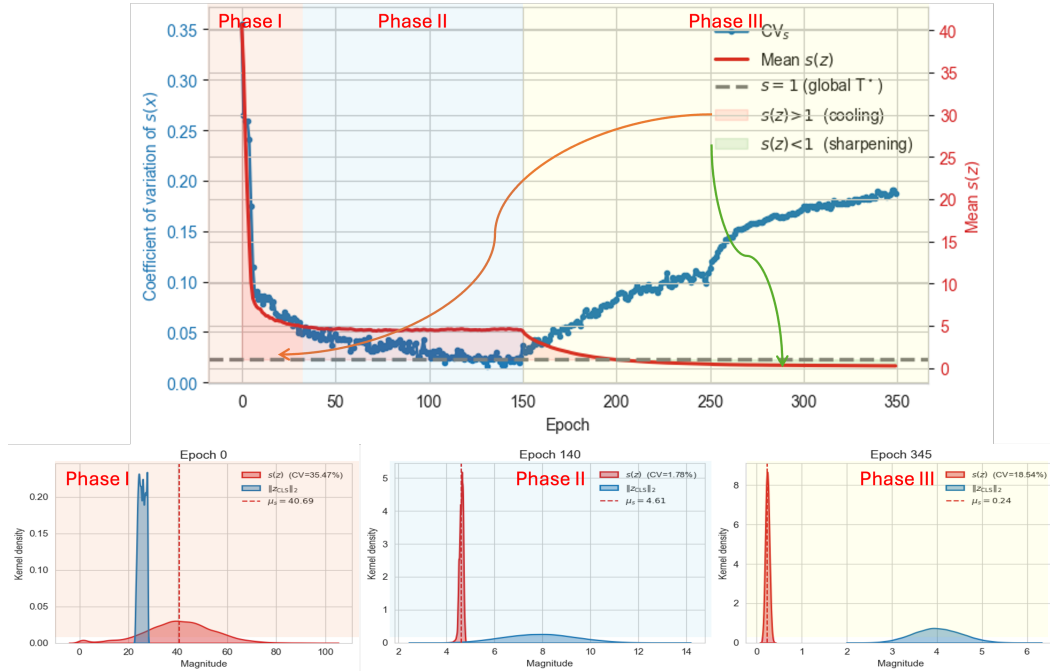


Figure 5: **Dynamics of the temperature head on ViT-224 (CIFAR-10).** *Top:* mean scale $s(z)$ (red, right axis) and coefficient of variation CV_s (blue, left axis). Grey dashed line marks the best global temperature T^* . Shaded bands denote cooling ($s > 1$) and sharpening ($s < 1$). *Bottom:* kernel-density estimates of $s(x)$ and $\|z_{CLS}\|_2$ at three epochs; legends report the mean μ and CV.

4.3 Temporal behaviour of CalAttn

Figure 5 traces the *per-sample* scale learned by CalAttn over 350 epochs (cosine schedule, $LR \times 0.1$ at epoch 150). Three distinct phases emerge:

Phase I – global alignment (epochs 0–30). The mean scale collapses from 40 to 4 while the coefficient of variation (CV) plummets from 0.35 to 0.05. The head therefore behaves like *classical temperature scaling*, quickly discovering a value that closely matches the post-hoc optimum T^* .

Phase II – selective sharpening (epochs 30–150). After a stable plateau the LR drop triggers a second descent of the mean: $s(z)$ crosses the neutral line $s = 1$ and enters the sharpening regime (green band). The CV bottoms out (≈ 0.02), indicating that most images still share a similar scale—CalAttn has not yet begun to exploit heteroscedasticity.

Phase III – heteroscedastic adaptation (epochs 150–350). Once the backbone has largely converged, the CV rises steadily to ≈ 0.18 : CalAttn now assigns *distinct* temperatures, cooling over-confident instances ($s > 1$) and sharpening under-confident ones ($s < 1$). Fig.5 confirm that the scale distribution widens while the CLS-norm distribution remains nearly stationary; the head therefore extracts additional calibration gain *without* perturbing the representation.

Take-away. CalAttn first replicates the best global T^* , then **learns instance-wise deviations** that track sample difficulty. The late-epoch rise of CV_s is thus *desirable*: it quantifies the head’s heteroscedastic expressiveness and correlates with the extra ECE reduction observed after epoch 150 (cf. Table 1). Crucially, the mean settling *below* one shows that its logits are not merely over-confident; some classes benefit from sharpening, that global temperature scaling cannot capture.

5 Related Work

Vision Transformers and their descendants. The seminal Vision Transformer (ViT) showed that a pure Transformer encoder—long dominant in NLP—can rival strong CNN baselines when trained on

sufficiently large image corpora [6]. Its heavy data requirements were soon alleviated by stronger regularisation and knowledge–distillation; **DeiT** reaches ResNet-50 accuracy on ImageNet using standard hardware and no extra data [7]. Parallel lines of work addressed the quadratic cost of full self-attention. The **Swin Transformer** introduces shifted window attention and a hierarchical pyramid, becoming the de-facto Transformer counterpart of FPNs for dense prediction [8]. Further refinements explore tokenisation [27], lightweight mixing [28], and positional priors [29]. Across this rapidly expanding family, however, the inference pipeline still terminates in a *fixed* soft-max layer; trustworthy confidence therefore hinges on post-hoc calibration.

Calibration for transformer classifiers. Classical calibration traces back to Platt scaling [30]; its modern successor, global temperature scaling (TS), remains the community’s work-horse [4]. Early studies focussed on CNNs, but the question of *Transformer* calibration has gained momentum only recently. Minderer et al. [5] report that ViTs are *often* better calibrated than CNNs, yet still benefit from a tuned T^* and reverses under distribution shift. Several losses have been proposed to side-step the global-temperature bottleneck. Adaptive focal variants increase the weight of poorly calibrated samples [18]; label smoothing can add a mild regularising signal [31]. Dual Focal Loss (DFL) enlarges the gap between the top two logits to reduce over-confidence [19]; Focal Calibration Loss (FCL) blends focal loss with a differentiable ECE surrogate [11]. Although effective, these objectives rely on *fixed* hyper-parameters and still apply the *same* scale to every image. Ensemble methods are also raised to improve a model’s calibration and robustness [32–35]. CTKD [36] and MKD [37] schedule a dynamic temperature during teacher-student distillation to balance hard and soft targets. CSM [25] is a diffusion-based re-annotation strategy for mixed-label samples to calibrate.

Gap addressed by Calibration Attention. Existing methods either (i) apply a single global temperature after training [4, 16, 18, 26] or (ii) prescribe static loss hyper-parameters [19, 11]. Neither class explicitly models the heteroscedastic uncertainty present across samples. Our **CalAttn** head learns an *instance-wise* temperature from the hidden CLS representation, integrates seamlessly with any ViT-style backbone, and is trained jointly with the task loss—bridging the remaining gap between predictive accuracy and reliable uncertainty. CalAttn is designed for vision transformers (ViT, DeiT, Swin) and relies on the presence of a global token (e.g. [CLS]) or equivalent GAP feature.

6 Conclusion

Post-hoc temperature–scaling remains the dominant fix for neural-network mis-calibration, yet its *single* global parameter cannot capture the wide variability in sample difficulty. CalAttn is designed for vision transformers (ViT, DeiT, Swin) and relies on the presence of a global token (e.g. [CLS]) or equivalent GAP feature. We have not yet explored extensions to CNNs, hybrid CNN-ViT models, or non-vision modalities. Adapting CalAttn to architectures without an explicit global token—by, for example, learning spatial pooling schemes—or to text and multimodal transformers is promising future work.

References

- [1] Alireza Mehrtaash, William M Wells, Clare M Tempany, Purang Abolmaesumi, and Tina Kapur. Confidence calibration and predictive uncertainty estimation for deep medical image segmentation. *IEEE transactions on medical imaging*, 39(12):3868–3878, 2020.
- [2] Di Feng, Ali Harakeh, Steven L Waslander, and Klaus Dietmayer. A review and comparative study on probabilistic object detection in autonomous driving. *IEEE Transactions on Intelligent Transportation Systems*, 23(8):9961–9980, 2021.
- [3] Wenhao Liang, Zhengyang Li, and Weitong Chen. Enhancing financial market predictions: Causality-driven feature selection. In *Advanced Data Mining and Applications*. Springer, 2024.
- [4] Chuan Guo, Geoff Pleiss, Yu Sun, and Kilian Q Weinberger. On calibration of modern neural networks. In *International Conference on Machine Learning*, pages 1321–1330. PMLR, 2017.
- [5] Matthias Minderer, Josip Djolonga, Rob Romijnders, Frances Hubis, Xiaohua Zhai, Neil Houlsby, Dustin Tran, and Mario Lucic. Revisiting the calibration of modern neural networks. *Advances in Neural Information Processing Systems*, 34:15682–15694, 2021.
- [6] Alexey Dosovitskiy, Lucas Beyer, Alexander Kolesnikov, Dirk Weissenborn, Xiaohua Zhai, Thomas Unterthiner, Mostafa Dehghani, Matthias Minderer, Georg Heigold, Sylvain Gelly, Jakob Uszkoreit, and Neil Houlsby. An image is worth 16x16 words: Transformers for image recognition at scale. In *International Conference on Learning Representations (ICLR)*, 2021.
- [7] Hugo Touvron, Matthieu Cord, Matthijs Douze, Francisco Massa, Alexandre Sablayrolles, and Hervé Jégou. Training data-efficient image transformers & distillation through attention. In *International Conference on Machine Learning*, pages 10347–10357. PMLR, 2021.
- [8] Ze Liu, Yutong Lin, Yue Cao, Han Hu, Yixuan Wei, Zheng Zhang, Stephen Lin, and Baining Guo. Swin transformer: Hierarchical vision transformer using shifted windows. In *Proceedings of the IEEE/CVF international conference on computer vision*, pages 10012–10022, 2021.
- [9] Tal Ridnik, Gilad Sharir, Emanuel Ben-Baruch, and Asaf Noy. Vit-calibrator: Decision stream calibration for vision transformers. *arXiv preprint arXiv:2302.02612*, 2023.
- [10] Xavier Glorot, Antoine Bordes, and Yoshua Bengio. Deep sparse rectifier neural networks. In *Proceedings of the fourteenth international conference on artificial intelligence and statistics*, pages 315–323. JMLR Workshop and Conference Proceedings, 2011.
- [11] Wenhao Liang, Chang Dong, Liangwei Zheng, Zhengyang Li, Wei Zhang, and Weitong Chen. Calibrating deep neural network using euclidean distance. *arXiv preprint arXiv:2410.18321*, 2024.
- [12] Jaroslaw Blasiok, Parikshit Gopalan, Lunjia Hu, and Preetum Nakkiran. When does optimizing a proper loss yield calibration? *Advances in Neural Information Processing Systems*, 36:72071–72095, 2023.
- [13] Muhammad Muzammal Naseer, Kanchana Ranasinghe, Salman H Khan, Munawar Hayat, Fahad Shahbaz Khan, and Ming-Hsuan Yang. Intriguing properties of vision transformers. *Advances in Neural Information Processing Systems*, 34:23296–23308, 2021.
- [14] Daquan Zhou, Zhiding Yu, Enze Xie, Chaowei Xiao, Animashree Anandkumar, Jiashi Feng, and Jose M Alvarez. Understanding the robustness in vision transformers. In *International conference on machine learning*, pages 27378–27394. PMLR, 2022.
- [15] Glenn W. Brier. Verification of forecasts expressed in terms of probability. *Monthly weather review*, 78(1): 1–3, 1950.
- [16] Aviral Kumar, Sunita Sarawagi, and Ujjwal Jain. Trainable calibration measures for neural networks from kernel mean embeddings. In *International Conference on Machine Learning*, pages 2805–2814. PMLR, 2018.
- [17] Christian Szegedy, Vincent Vanhoucke, Sergey Ioffe, Jon Shlens, and Zbigniew Wojna. Rethinking the inception architecture for computer vision. In *cvpr*, 2016.
- [18] Jishnu Mukhoti, Viveka Kulharia, Amartya Sanyal, Stuart Golodetz, Philip Torr, and Puneet Dokania. Calibrating deep neural networks using focal loss. *Advances in Neural Information Processing Systems*, 33:15288–15299, 2020.
- [19] Linwei Tao, Minjing Dong, and Chang Xu. Dual focal loss for calibration. In *International Conference on Machine Learning (ICML)*, 2023.

- [20] Glenn W. Brier. Verification of forecasts expressed in terms of probability. *Monthly Weather Review*, 78 (1):1–3, 1950.
- [21] Jishnu Mukhoti, Viveka Kulharia, Amartya Sanyal, Stuart Golodetz, Philip HS Torr, and Puneet K Dokania. Focal calibration. https://github.com/torrvision/focal_calibration, 2020. Accessed: 2024-10-08.
- [22] Deng-Bao Wang, Lei Feng, and Min-Ling Zhang. Rethinking calibration of deep neural networks: Do not be afraid of overconfidence. *Advances in Neural Information Processing Systems*, 34:11809–11820, 2021.
- [23] Jarosław Błasiok and Preetum Nakkiran. Smooth ece: Principled reliability diagrams via kernel smoothing. *arXiv preprint arXiv:2309.12236*, 2023.
- [24] Błasiok, Jarosław and Nakkiran, Preetum. ml-calibration. <https://github.com/apple/ml-calibration>, 2024. Accessed: 2024-10-08.
- [25] Haoyang Luo, Linwei Tao, Minjing Dong, and Chang Xu. Beyond one-hot labels: Semantic mixing for model calibration. *arXiv preprint arXiv:2504.13548*, 2025.
- [26] Tom Joy, Francesco Pinto, Ser-Nam Lim, Philip HS Torr, and Puneet K Dokania. Sample-dependent adaptive temperature scaling for improved calibration. In *Proceedings of the AAAI Conference on Artificial Intelligence*, volume 37, pages 14919–14926, 2023.
- [27] Li Yuan, Yunpeng Chen, Tao Wang, Weihao Yu, Yujun Shi, Zi-Hang Jiang, Francis EH Tay, Jiashi Feng, and Shuicheng Yan. Tokens-to-token vit: Training vision transformers from scratch on imagenet. In *Proceedings of the IEEE/CVF international conference on computer vision*, pages 558–567, 2021.
- [28] Zhengsu Chen, Lingxi Xie, Jianwei Niu, Xuefeng Liu, Longhui Wei, and Qi Tian. Visformer: The vision-friendly transformer. In *Proceedings of the IEEE/CVF international conference on computer vision*, pages 589–598, 2021.
- [29] Zihang Dai, Hanxiao Liu, Quoc V Le, and Mingxing Tan. Coatnet: Marrying convolution and attention for all data sizes. *Advances in neural information processing systems*, 34:3965–3977, 2021.
- [30] John Platt et al. Probabilistic outputs for support vector machines and comparisons to regularized likelihood methods. *Advances in large margin classifiers*, 10(3):61–74, 1999.
- [31] Rafael Müller, Simon Kornblith, and Geoffrey E. Hinton. When does label smoothing help? *Advances in neural information processing systems*, 32, 2019.
- [32] Yarín Gal and Zoubin Ghahramani. Dropout as a bayesian approximation: Representing model uncertainty in deep learning. In *international conference on machine learning*, pages 1050–1059. PMLR, 2016.
- [33] Balaji Lakshminarayanan, Alexander Pritzel, and Charles Blundell. Simple and scalable predictive uncertainty estimation using deep ensembles. *Advances in neural information processing systems*, 30, 2017.
- [34] Yaniv Ovadia, Emily Fertig, Jie Ren, Zachary Nado, David Sculley, Sebastian Nowozin, Joshua Dillon, Balaji Lakshminarayanan, and Jasper Snoek. Can you trust your model’s uncertainty? evaluating predictive uncertainty under dataset shift. *Advances in neural information processing systems*, 32, 2019.
- [35] Yeming Wen, Dustin Tran, and Jimmy Ba. Batchensemble: an alternative approach to efficient ensemble and lifelong learning. *arXiv preprint arXiv:2002.06715*, 2020.
- [36] Zheng Li, Xiang Li, Lingfeng Yang, Borui Zhao, Renjie Song, Lei Luo, Jun Li, and Jian Yang. Curriculum temperature for knowledge distillation. In *Proceedings of the AAAI Conference on Artificial Intelligence*, volume 37, pages 1504–1512, 2023.
- [37] Jihao Liu, Boxiao Liu, Hongsheng Li, and Yu Liu. Meta knowledge distillation, 2022. URL <https://arxiv.org/abs/2202.07940>.
- [38] Bingyuan Liu, Ismail Ben Ayed, Adrian Galdran, and Jose Dolz. The devil is in the margin: Margin-based label smoothing for network calibration. In *Proceedings of the IEEE/CVF Conference on Computer Vision and Pattern Recognition*, pages 80–88, 2022.

A Notation table for the Calibration-Attention

All notations in our work define in Table 3.

Table 3: Notation and abbreviations used throughout the paper. Shapes refer to vision experiments.

Symbol / op.	Meaning	Shape / type
B	Mini-batch size	—
C	Number of classes	—
N	Number of image patches	—
L	Transformer encoder depth	—
d	Token / CLS embedding dimension	e.g. 384, 768
H, W	Input image height / width	e.g. 32, 224
\mathbf{x}	Input image tensor	$(B, 3, H, W)$
$\text{patch_embed}(\cdot)$	Linear projection of image patches	—
[CLS]	Learned classification token	$(1, d)$
$\mathbf{z}_{\text{CLS}} (= \mathbf{z})$	Final CLS embedding (after encoder & LN)	(B, d)
$W_{\text{cls}}, b_{\text{cls}}$	Weights / bias of classifier head	$d \times C, C$
ℓ	Raw logits $\ell = W_{\text{cls}}\mathbf{z} + b_{\text{cls}}$	(B, C)
h	Hidden width of Calibration MLP	default 128
\mathbf{h}	Hidden activation $\text{GELU}(\mathbf{z}W_c^{(1)})$	(B, h)
Calibration Head	Two-layer MLP: $\mathbf{z} \xrightarrow{\text{FC}(d \rightarrow h)} \xrightarrow{\text{GELU}} \xrightarrow{\text{FC}(h \rightarrow 1)} \xrightarrow{\text{Softplus}} s(\mathbf{z})$	—
$s(\mathbf{z})$	Per-sample temperature	$(B, 1)$
ε	Numerical safety term (10^{-6})	scalar
$\tilde{\ell}$	Scaled logits $\ell / (s(\mathbf{z}) + \varepsilon)$	(B, C)
$\hat{\mathbf{y}}$	Probabilities $\text{softmax}(\tilde{\ell})$	(B, C)
\mathbf{e}_y	One-hot ground-truth label	(B, C)
\mathcal{L}_{CE}	Cross-entropy loss	scalar
$\mathcal{L}_{\text{Brier}}$	Brier penalty $\ \hat{\mathbf{y}} - \mathbf{e}_y\ _2^2$	scalar
λ	Weight on Brier term (default 0.1)	scalar
ECE, AdaECE, smCE, Classwise-ECE	Calibration metrics	—
Operators / special symbols		
\boxplus	Element-wise addition (broadcast) with positional encoding	binary op.
$\ \cdot\ _2$	Euclidean (L2) norm	scalar
$\text{LN}(\cdot)$	Layer Normalisation	function
σ_i	i -th component of the soft-max	scalar prob.
GELU, Softplus	Non-linearities	—

B Calibration Metrics

A classifier is *perfectly calibrated* when the predictive confidence matches the empirical accuracy, i.e. $\Pr(y = \hat{y} \mid \hat{p} = p) = p$ for every $p \in [0, 1]$. All metrics below measure the deviation from this ideal diagonal.

Histogram-based metrics. Let $\hat{p}_i = \max_c \hat{y}_{ic}$ be the top-class confidence for sample i and $\mathbb{1}(\cdot)$ the indicator function. Partition the unit interval into M bins and define

$$\text{acc}(B_m) = \frac{1}{|B_m|} \sum_{i \in B_m} \mathbb{1}(\hat{y}_i = y_i), \quad \text{conf}(B_m) = \frac{1}{|B_m|} \sum_{i \in B_m} \hat{p}_i. \quad (7)$$

With $N = \sum_m |B_m|$ the classic metrics become

$$\text{ECE} = \sum_{m=1}^M \frac{|B_m|}{N} |\text{acc}(B_m) - \text{conf}(B_m)|, \quad (8)$$

$$\text{MCE} = \max_m |\text{acc}(B_m) - \text{conf}(B_m)|, \quad (9)$$

$$\text{AdaECE} = \sum_{m=1}^M \frac{|B_m|}{N} |\text{acc}(B_m) - \text{conf}(B_m)| \quad (\text{adaptive binning}), \quad (10)$$

$$\text{ClassECE} = \frac{1}{K} \sum_{k=1}^K \sum_{m=1}^M \frac{|B_{km}|}{N_k} |\text{acc}(B_{km}) - \text{conf}(B_{km})|. \quad (11)$$

Smooth ECE (SMECE). Hard bin edges can mask fine-grained mis-calibration. Błasiok and Nakkiran [23] replace binning with kernel smoothing. Using a Gaussian kernel $K_h(t) = \exp(-t^2/2h^2)$ and bandwidth h :

$$\widehat{\text{acc}}(\hat{p}_i) = \frac{\sum_j K_h(\hat{p}_i - \hat{p}_j) \mathbb{1}(\hat{y}_j = y_j)}{\sum_j K_h(\hat{p}_i - \hat{p}_j)}, \quad \text{smECE} = \frac{1}{N} \sum_{i=1}^N |\widehat{\text{acc}}(\hat{p}_i) - \hat{p}_i|. \quad (12)$$

The kernel view removes bin-edge artefacts and yields a *differentiable* objective, which underpins recent calibration losses such as FCL[11] and the proposed CalAttn head.⁴

Interpretation in this work. ECE, MCE, AdaECE and Classwise-ECE are intuitive and readily visualised via reliability diagrams, while SMECE offers a high-resolution, bin-free perspective. We report **all five** scores (Sec. 3) and show that CalAttn lowers each of them— including the stringent SMECE—demonstrating genuine, sample-wise calibration improvements beyond coarse histogram effects.

C Architectural Differences

We show differences between the vanilla Vision Transformer and our proposed Calibration-Attention variant in Table 4.

Table 4: Architectural differences between the vanilla Vision Transformer and our proposed Calibration-Attention variant.

Component	Baseline ViT	ViT+Calibration Attention
Extra module	—	Calibration Head — a two-layer MLP attached to the CLS embedding
Output of the module	—	Strictly positive scale $s(\mathbf{z})$ (initially ≈ 1.0)
Logits fed to Soft-max	ℓ	$\ell/s(\mathbf{z})$ (sample-specific cooling / sharpening)
Loss function	Cross-entropy only	Cross-entropy + small Brier term (differentiable calibration surrogate)
Post-hoc temperature search	Required	Not needed — network learns $s(\mathbf{z})$ end-to-end
Extra parameters	0	<0.1% of total (two small fully-connected layers)

D Vision Transformer + Calibration Attention: Forward Steps

1. Patch embedding.

$$\mathbf{X}_{\text{patch}} = \text{reshape}(\text{Conv}_{3 \rightarrow D}^{P,P}(\mathbf{x}), N, D) \in \mathbb{R}^{N \times D}$$

⁴We follow Błasiok and Nakkiran [23] and fix $h = 0.05$ for all experiments.

2. Class token and positions.

$$\mathbf{z}^{(0)} = [\mathbf{z}_{\text{cls}} \ \mathbf{X}_{\text{patch}}] \boxplus \mathbf{E}_{\text{pos}} \in \mathbb{R}^{(N+1) \times D} \quad (\text{init})$$

3. Encoder blocks (for $\ell = 1..L$). Each block contains multi-head self-attention (MSA) followed by a feed-forward network (MLP) with residual connections and LayerNorm:

$$\begin{aligned} \mathbf{u}^{(\ell)} &= \text{LN}(\mathbf{z}^{(\ell-1)}), \\ \mathbf{a}^{(\ell)} &= \text{MSA}(\mathbf{u}^{(\ell)}) = \bigoplus_{k=1}^h \underbrace{\text{softmax}\left(\frac{\mathbf{Q}_k \mathbf{K}_k^\top}{\sqrt{D/h}}\right)}_{\text{head } k} \mathbf{V}_k \mathbf{W}_o, \\ \mathbf{z}^{(\ell)} &= \mathbf{z}^{(\ell-1)} + \mathbf{a}^{(\ell)}, \\ \mathbf{v}^{(\ell)} &= \text{LN}(\mathbf{z}^{(\ell)}), \\ \mathbf{m}^{(\ell)} &= \text{MLP}(\mathbf{v}^{(\ell)}) = \sigma(\mathbf{v}^{(\ell)} \mathbf{W}_1) \mathbf{W}_2, \\ \mathbf{z}^{(\ell)} &= \mathbf{z}^{(\ell)} + \mathbf{m}^{(\ell)}. \end{aligned}$$

4. Calibration head (instance-wise temperature).

$$\begin{aligned} \mathbf{h} &= \text{GELU}(\mathbf{z}_0^{(L)} \mathbf{W}_c^{(1)}) \in \mathbb{R}^{1 \times H}, \\ s &= \text{softplus}(\mathbf{h} \mathbf{W}_c^{(2)} + b_c) + \varepsilon \in \mathbb{R}_{>0}, \\ \boldsymbol{\ell} &= \frac{\mathbf{z}_0^{(L)} \mathbf{W}_{\text{cls}}}{s} \in \mathbb{R}^C, \\ \hat{\mathbf{y}} &= \text{softmax}(\boldsymbol{\ell}). \end{aligned}$$

5. Loss.

$$\mathcal{L} = -\log \hat{y}_y + \lambda \|\hat{\mathbf{y}} - \mathbf{e}_y\|_2^2 \quad (\lambda = 0.1).$$

E Proof that CalAttn converges to the optimal temperature

Let $\boldsymbol{\ell}$ be the raw logits and $\tilde{\boldsymbol{\ell}} = \boldsymbol{\ell}/s$ the scaled logits. With $\hat{\mathbf{y}} = \text{softmax}(\tilde{\boldsymbol{\ell}})$ and ground-truth one-hot \mathbf{e}_y , the loss is

$$\mathcal{L} = -\log \hat{y}_y + \lambda \|\hat{\mathbf{y}} - \mathbf{e}_y\|_2^2.$$

The derivative w.r.t. s is⁵

$$\frac{\partial \mathcal{L}}{\partial s} = (\hat{y}_y - 1) \frac{\ell_y - \sum_j \hat{y}_j \ell_j}{s} + 2\lambda \sum_c (\hat{y}_c - \mathbf{e}_{yc}) \hat{y}_c (1 - \hat{y}_c) \frac{\ell_c - \sum_j \hat{y}_j \ell_j}{s}.$$

Setting $\partial \mathcal{L} / \partial s = 0$ and rearranging yields

$$s^* = \frac{\ell_y - \sum_j \hat{y}_j \ell_j}{\ell_y^{\text{opt}} - \sum_j \hat{y}_j^{\text{opt}} \ell_j},$$

where ‘‘opt’’ denotes the soft-max that exactly matches empirical accuracy, $\hat{y}_y^{\text{opt}} = \mathbf{1}(\hat{y} = y)$. Hence s^* equals the *temperature* that aligns confidence with correctness for that sample—i.e. the per-instance optimum of temperature scaling.

F AdaECE and Classwise-ECE

We extend the metrics to AdaECE and Classwise-ECE in Tables 5 and 6.

⁵See Guo et al. [4] for the CE part; the Brier term is similar.

Table 5: \downarrow AdaECE (%) for methods both before and after applying temperature scaling.

Dataset	Model	Weight Decay [4]		Brier Loss [15]		MMCE [16]		Label Smooth [17]		Focal Loss - 53 [18]		Dual Focal [19]		CE + BS [4, 20]	
		Pre T	Post T	Pre T	Post T	Pre T	Post T	Pre T	Post T	Pre T	Post T	Pre T	Post T	Pre T	Post T
CIFAR-100	ResNet-50	17.99	3.38(2.2)	5.46	4.24(1.1)	15.05	3.42(1.9)	6.72	5.37(1.1)	5.64	2.84(1.1)	8.79	2.27(1.3)	14.41	2.38(1.60)
	ResNet-110	19.28	6.27(2.3)	6.51	3.75(1.2)	18.83	4.86(2.3)	9.68	8.11(1.3)	10.90	4.13(1.3)	11.64	4.48(1.3)	19.35	3.51(1.80)
	Wide-ResNet-26-10	15.16	3.23(2.1)	4.08	3.11(1.1)	13.55	3.83(2.0)	3.73	3.73(1.0)	2.40	2.38(1.1)	5.36	2.38(1.2)	6.59	5.19(1.20)
	DenseNet-121	19.07	3.82(2.2)	3.92	2.41(1.1)	17.37	3.07(2.0)	8.62	5.92(1.1)	3.35	1.80(1.1)	6.69	1.69(1.2)	16.09	3.04(1.60)
	ViT ₂₂₄	13.11	3.34(1.30)	2.58	2.56(1.10)	11.51	2.33(1.30)	3.77	2.32(1.10)	5.07	3.41(1.10)	3.56	3.56(1.00)	6.55	3.54(1.50)
	ViT ₂₂₄ +CalAttn(Ours)	8.25	1.83(1.20)	1.93	2.56(1.10)	9.04	2.11(1.20)	2.12	2.12(1.00)	2.60	2.60(1.00)	3.73	2.07(1.10)	4.01	1.47(1.10)
	DeiT _{small}	7.46	3.57(1.10)	2.26	2.26(1.00)	7.88	2.35(1.20)	1.67	1.67(1.00)	3.18	3.18(1.00)	2.01	2.01(1.00)	5.93	2.85(1.40)
	DeiT _{small} +CalAttn(Ours)	6.87	1.04(1.20)	1.92	2.41(1.10)	6.51	1.34(1.20)	1.67	1.67(1.00)	3.08	3.08(1.00)	3.05	2.47(1.10)	4.36	1.73(1.10)
	Swin _{small}	3.58	2.52(0.90)	2.60	2.60(1.00)	3.54	2.75(0.90)	9.29	2.56(0.80)	10.71	2.71(0.80)	8.24	3.16(0.80)	4.07	2.93(1.20)
	Swin _{small} +CalAttn(Ours)	2.20	2.20(1.00)	2.95	2.24(1.10)	1.97	1.97(1.00)	6.55	2.65(0.90)	6.10	3.16(0.90)	3.85	3.22(0.90)	1.75	1.75(1.00)
CIFAR-10	ResNet-50	4.22	2.11(2.5)	1.85	1.34(1.1)	4.67	2.01(2.6)	4.28	3.20(0.9)	1.64	1.64(1.0)	1.28	1.28(1.0)	5.69	1.98(1.90)
	ResNet-110	4.78	2.42(2.6)	2.52	1.72(1.2)	5.21	2.66(2.8)	4.57	3.62(0.9)	1.76	1.32(1.1)	1.69	1.42(1.1)	6.23	2.88(1.90)
	Wide-ResNet-26-10	3.22	1.62(2.2)	1.94	1.94(1.0)	3.58	1.83(2.2)	4.58	2.55(0.8)	1.84	1.63(0.9)	3.16	1.20(0.8)	3.41	1.76(1.50)
	DenseNet-121	4.69	2.28(2.4)	1.84	1.84(1.0)	4.97	2.69(2.4)	4.60	3.36(0.9)	1.58	1.62(0.9)	0.79	1.32(0.9)	5.12	3.25(1.60)
	ViT ₂₂₄	7.39	1.37(1.30)	2.27	2.27(1.00)	3.47	1.23(1.10)	1.58	1.58(1.00)	8.77	2.24(0.70)	4.16	2.27(0.90)	3.58	2.68(1.40)
	ViT ₂₂₄ +CalAttn(Ours)	4.74	1.62(1.20)	2.68	1.14(1.10)	4.35	1.78(1.20)	2.74	1.41(0.90)	9.96	2.30(0.70)	4.52	3.09(0.90)	2.17	1.86(1.10)
	DeiT _{small}	4.41	1.52(1.20)	1.97	1.97(1.00)	6.01	1.84(1.20)	1.66	1.66(1.00)	10.62	3.17(0.70)	5.11	3.00(0.80)	2.97	1.83(1.30)
	DeiT _{small} +CalAttn(Ours)	4.08	1.95(1.10)	1.99	1.59(1.10)	3.48	1.40(1.10)	2.20	2.20(1.00)	9.91	1.73(0.70)	4.20	2.87(0.90)	1.95	1.39(1.10)
	Swin _{small}	1.27	2.00(0.90)	1.77	1.77(1.00)	1.86	2.42(0.90)	6.67	1.41(0.80)	15.69	2.28(0.60)	8.40	2.57(0.70)	1.66	1.40(1.20)
	Swin _{small} +CalAttn(Ours)	1.66	1.66(1.00)	1.17	1.17(1.00)	0.97	0.97(1.00)	5.94	1.56(0.80)	14.98	1.56(0.60)	7.40	2.47(0.80)	0.88	0.88(1.00)
MNIST	ViT ₂₂₄	2.97	1.15(0.90)	48.83	6.07(8.70)	19.96	5.28(2.10)	12.82	8.53(1.50)	24.06	2.41(1.40)	18.12	5.07(2.30)	5.34	1.08(0.80)
	ViT ₂₂₄ +CalAttn(Ours)	2.65	0.80(0.90)	3.12	0.77(0.90)	3.89	1.08(0.80)	8.29	1.15(0.70)	7.04	1.10(0.40)	18.38	1.54(0.50)	0.74	0.40(0.90)
	DeiT _{small}	2.85	1.11(0.90)	28.36	3.06(3.20)	4.53	0.98(0.80)	8.69	0.97(0.70)	21.72	2.26(0.50)	8.96	1.87(0.70)	4.48	1.04(0.80)
	DeiT _{small} +CalAttn(Ours)	1.17	1.17(1.00)	1.08	1.04(0.90)	2.22	1.02(0.90)	6.20	1.33(0.80)	18.28	1.81(0.50)	15.90	2.38(0.60)	0.91	0.91(1.00)
	Swin _{small}	3.64	3.21(1.10)	1.12	0.38(0.90)	1.24	0.50(0.90)	7.99	1.21(0.70)	7.08	0.35(0.50)	5.04	0.37(0.90)	0.46	0.46(1.00)
Swin _{small} +CalAttn(Ours)	0.84	0.39(1.20)	0.76	0.32(0.90)	1.19	0.46(0.90)	6.59	1.01(0.70)	11.74	0.75(0.50)	8.79	0.40(0.50)	0.85	0.42(0.90)	
Tiny-ImageNet	ViT ₂₂₄	4.36	1.73(1.10)	4.40	1.67(1.10)	4.96	2.39(1.20)	2.09	2.28(1.10)	3.23	2.23(1.10)	2.50	2.68(1.10)	1.44	1.39(1.10)
	ViT ₂₂₄ +CalAttn(Ours)	22.11	3.01(1.90)	9.18	0.85(1.30)	19.84	3.02(1.80)	2.05	1.98(1.10)	1.68	1.23(1.10)	13.57	1.10(1.40)	1.01	0.78(1.10)
	DeiT _{small}	13.04	2.25(1.40)	2.38	2.04(1.10)	13.66	1.37(1.50)	1.71	1.71(1.00)	10.26	2.39(1.70)	9.37	1.86(1.50)	1.43	1.29(1.10)
	DeiT _{small} +CalAttn(Ours)	2.12	1.77(1.40)	2.26	1.47(1.20)	2.61	1.07(1.50)	2.29	1.35(1.10)	2.39	1.26(1.30)	1.86	1.41(1.30)	0.95	0.83(1.20)
	Swin _{small}	3.48	2.54(0.90)	1.05	0.54(0.90)	2.15	2.15(1.00)	4.98	2.44(0.90)	4.66	2.69(0.90)	4.96	2.62(0.90)	0.91	0.91(1.00)
Swin _{small} +CalAttn(Ours)	2.84	1.63(1.10)	0.84	1.12(1.10)	1.57	1.57(1.00)	2.62	2.62(1.00)	2.37	2.37(1.00)	2.29	2.29(1.00)	0.82	0.24(0.90)	

Table 6: \downarrow Classwise-ECE (%) for methods both before and after applying temperature scaling.

Dataset	Model	Weight Decay [4]		Brier Loss [15]		MMCE [16]		Label Smooth [17]		Focal Loss - 53 [18]		Dual Focal [19]		CE + BS [4, 20]	
		Pre T	Post T	Pre T	Post T	Pre T	Post T	Pre T	Post T	Pre T	Post T	Pre T	Post T	Pre T	Post T
CIFAR-100	ResNet-50	0.39	0.22(2.2)	0.21	0.22(1.1)	0.34	0.22(1.9)	0.21	0.22(1.1)	0.21	0.20(1.1)	0.24	0.22(1.3)	0.34	0.23(1.60)
	ResNet-110	0.42	0.21(2.3)	0.22	0.23(1.2)	0.41	0.22(2.3)	0.25	0.23(1.3)	0.27	0.22(1.3)	0.28	0.21(1.3)	0.43	0.23(1.80)
	Wide-ResNet-26-10	0.34	0.21(2.1)	0.19	0.20(1.1)	0.31	0.21(2.0)	0.20	0.20(1.0)	0.18	0.20(1.1)	0.19	0.20(1.2)	0.33	0.30(1.20)
	DenseNet-121	0.42	0.22(2.2)	0.21	0.21(1.1)	0.39	0.23(2.0)	0.23	0.21(1.1)	0.20	0.21(1.1)	0.22	0.21(1.2)	0.37	0.25(1.60)
	ViT ₂₂₄	0.43	0.26(1.30)	0.29	0.28(1.10)	0.40	0.26(1.30)	0.27	0.25(1.10)	0.33	0.29(1.10)	0.28	0.28(1.00)	0.30	0.27(1.50)
	ViT ₂₂₄ +CalAttn(Ours)	0.34	0.27(1.20)	0.35	0.34(1.10)	0.36	0.29(1.20)	0.28	0.28(1.00)	0.30	0.30(1.00)	0.29	0.26(1.10)	0.29	0.26(1.10)
	DeiT _{small}	0.33	0.28(1.10)	0.28	0.28(1.00)	0.33	0.26(1.20)	0.26	0.26(1.00)	0.29	0.29(1.00)	0.27	0.27(1.00)	0.33	0.30(1.40)
	DeiT _{small} +CalAttn(Ours)	0.33	0.27(1.20)	0.36	0.36(1.10)	0.32	0.26(1.20)	0.28	0.28(1.00)	0.29	0.29(1.00)	0.28	0.26(1.10)	0.32	0.29(1.10)
	Swin _{small}	0.28	0.28(0.90)	0.35	0.35(1.00)	0.27	0.27(0.90)	0.33	0.30(0.80)	0.33	0.29(0.80)	0.33	0.31(0.80)	0.30	0.29(1.20)
	Swin _{small} +CalAttn(Ours)	0.28	0.28(1.00)	0.41	0.40(1.10)	0.27	0.27(1.00)	0.30	0.28(0.90)	0.28	0.27(0.90)	0.27	0.28(0.90)	0.27	0.27(1.00)
CIFAR-10	ResNet-50	0.87	0.37(2.5)	0.46	0.39(1.1)	0.97	0.55(2.6)	0.80	0.54(0.9)	0.41	0.41(1.0)	0.45	0.45(1.0)	1.18	0.58(1.90)
	ResNet-110	1.00	0.54(2.6)	0.55	0.46(1.2)	1.08	0.60(2.8)	0.75	0.50(0.9)	0.48	0.46(1.1)	0.46	0.52(1.1)	1.31	0.68(1.90)
	Wide-ResNet-26-10	0.68	0.34(2.2)	0.37	0.37(1.0)	0.77	0.41(2.2)	0.95	0.37(0.8)	0.44	0.34(0.9)	0.82	0.33(0.8)	1.24	1.12(1.50)
	DenseNet-121	0.98	0.54(2.4)	0.43	0.43(1.0)	1.02	0.53(2.4)	0.75	0.48(0.9)	0.43	0.41(0.9)	0.40	0.41(0.9)	1.17	0.58(1.60)
	ViT ₂₂₄	1.68	0.78(1.30)	1.15	1.15(1.00)	0.97	0.70(1.10)	0.73	0.73(1.00)	1.76	1.32(0.70)	0.96	0.89(0.90)	1.44	1.32(1.40)
	ViT ₂₂₄ +CalAttn(Ours)	1.33	0.85(1.20)	1.45	1.29(1.10)	1.42	0.99(1.20)	1.25	1.05(0.90)	2.09	1.33(0.70)	1.34	1.29(0.90)	1.13	1.10(1.10)
	DeiT _{small}	1.24	0.74(1.20)	1.41	1.41(1.00)	1.35	0.71(1.20)	0.88	0.88(1.00)	2.12	1.05(0.70)	1.19	1.08(0.80)	1.26	0.97(1.30)
	DeiT _{small} +CalAttn(Ours)	1.16	0.89(1.10)	0.93	0.86(1.10)	1.13	0.91(1.10)	0.97	0.97(1.00)	1.98	1.14(0.70)	1.21	1.16(0.90)	0.93	0.86(1.10)
	Swin _{small}	0.93	1.05(0.90)	1.31	1.31(1.00)	0.76	0.92(0.90)	1.66	0.88(0.80)	3.17	1.15(0.60)	1.82	1.15(0.70)	1.14	0.78(1.20)
	Swin _{small} +CalAttn(Ours)	0.86	0.86(1.00)	0.96	0.96(1.00)	0.92	0.92(1.00)	1.36	0.82(0.80)	2.94	0.89(0.60)	1.65	1.08(0.80)	0.69	0.69(1.00)
MNIST	ViT ₂₂₄	1.06	0.91(0.90)	11.83	4.11(8.70)	6.23	5.26(2.10)	5.91	5.78(1.50)	5.59	5.84(1.40)	5.83	4.73(2.30)	1.34	0.85(0.80)
	ViT ₂₂₄ +CalAttn(Ours)	1.24	1.09(0.90)	1.26	1.08(0.90)	1.25	0.93(0.80)	1.84	0.64(0.70)	4.92	1.21(0.40)	4.03	1.40(0.50)	0.43	0.38(0.80)
	DeiT _{small}	1.20	1.02(0.90)	8.37	5.63(3.20)	1.63	1.21(0.80)	2.27	1.28(0.70)	4.58	1.49(0.50)	2.95	2.00(0.70)	1.32	1.11(0.80)
	DeiT _{small} +CalAttn(Ours)	1.01	1.01(1.00)	1.03	1.03(1.00)	1.17	1.03(0.90)	1.74	1.04(0.80)	4.32	1.75(0.50)	3.88	1.36(0.60)	0.53	0.44(0.90)
	Swin _{small}	0.38	0.30(1.10)	0.53	0.43(0.90)	0.71	0.63(0.90)	2.21	1.01(0.70)	1.60	0.36(0.50)	1.29	0.53(0.60		

G Impact of Calibration on Model Size

Table 7: Disk footprint of the saved .pth checkpoints. The last column shows the *absolute* increase brought by CalAttn.

Dataset	Backbone	Variant	Size (MB)	Δ (MB)
CIFAR-10	ViT ₂₂₄	baseline	327.38	—
		+ CalAttn (ours)	327.76	+0.38
	DeiT _{small}	baseline	82.72	—
		+ CalAttn (ours)	82.91	+0.19
	Swin _{small}	baseline	186.16	—
		+ CalAttn (ours)	186.54	+0.38
CIFAR-100	ViT ₂₂₄	baseline	327.64	—
		+ CalAttn (ours)	328.02	+0.38
	DeiT _{small}	baseline	82.85	—
		+ CalAttn (ours)	83.04	+0.19
	Swin _{small}	baseline	186.42	—
		+ CalAttn (ours)	186.80	+0.38

H Classification Error

Table 8: Top-1 error (% , lower is better) on CIFAR-10 / CIFAR-100 test set (Results report on 350 epochs by Cross Entropy.).

Back-bone	CIFAR-10		CIFAR-100	
	baseline	+CalAttn	baseline	+CalAttn
ViT ₂₂₄	33.9	32.2	40.8	40.4
DeiT _{small}	30.6	30.5	36.1	35.9
Swin _{small}	25.5	25.2	33.3	32.8

I Robustness on OoD Data Shift

Table 9: Robustness on OoD Dataset Shift. \uparrow AUROC (%) for shifting CIFAR-10 (in-distribution) to SVHN and CIFAR-10-C (OoD).

Dataset	Model	Weight Decay [4]	Brier Loss [15]	MMCE [16]	Label Smooth [17]	Focal Loss-53 [18]	Dual Focal [19]	CE+BS [4, 20]
CIFAR-10 \rightarrow SVHN	ViT ₂₂₄	74.48	63.03	68.56	68.42	70.11	70.24	—
	ViT ₂₂₄ +CalAttn	70.03	61.11	69.32	68.75	67.43	67.82	75.36
	DeiT _{small}	73.72	63.74	74.53	74.06	70.43	69.09	—
	DeiT _{small} +CalAttn	72.40	57.21	70.31	67.24	66.38	63.65	66.93
	Swin _{small}	70.43	52.34	72.45	75.46	67.67	72.12	—
	Swin _{small} +CalAttn	69.42	68.53	66.16	68.92	60.98	70.07	67.36
CIFAR-10 \rightarrow CIFAR-10-C	ViT ₂₂₄	52.86	52.19	52.85	51.53	52.33	51.71	—
	ViT ₂₂₄ +CalAttn	52.40	52.35	52.60	52.08	52.24	51.97	53.21
	DeiT _{small}	52.19	51.93	52.61	51.80	52.47	52.35	—
	DeiT _{small} +CalAttn	52.50	51.86	52.34	52.01	52.07	51.93	53.27
	Swin _{small}	59.71	54.60	67.48	61.57	60.68	58.59	—
	Swin _{small} +CalAttn	61.69	57.84	59.25	64.81	69.61	63.81	68.27

J Calibration on CalAttn

J.1 ImageNet-1K Results

We fine-tune each model on ImageNet-1K for 350 epochs and report Top-1 accuracy, Expected Calibration Error (ECE), and Adaptive ECE (AECCE). CSM results are taken from [25].

Table 10: Ablation on CalAttn input features. Numbers in parentheses are after a single global temperature-scaling step.

Dataset	Model	Method	ECE (%)	AECE	CECE	SmoothECE
CIFAR-100	DeiT-S	CE	7.46(3.54)	7.46(3.57)	0.33(0.28)	7.45(3.48)
		CE+BS (w/o CalAttn)	4.30(2.39)	4.26(2.44)	0.31(0.27)	4.20(2.44)
		CE+BS+CalAttn(CLS)	6.87(1.48)	6.87(1.04)	0.33(0.26)	6.87(1.59)
		CE+BS+CalAttn(Patch Mean)	4.38 (1.03)	4.41 (1.32)	0.27(0.26)	4.38 (1.36)
		CE+BS+CalAttn(Concat)	7.29(0.91)	7.29(0.91)	0.33(0.27)	7.28(1.28)
	ViT-224	CE	7.39(1.68)	13.11(3.34)	0.43(0.26)	13.07(3.32)
		CE+BS	7.96(2.01)	8.96(2.24)	0.34(0.26)	8.96(1.97)
		CE+BS+CalAttn(CLS)	4.76(1.38)	8.25(1.83)	0.33(0.25)	8.24(1.92)
		CE+BS+CalAttn(Patch Mean)	2.46 (2.46)	2.18 (2.18)	0.26(0.26)	2.32 (2.32)
		CE+BS+CalAttn(Concat)	11.56(1.98)	11.56(2.02)	0.40(0.27)	11.55(2.01)
Swin-S	CE	3.51(2.46)	3.58(2.52)	0.28(0.28)	3.44(2.44)	
	CE+BS	3.21(3.21)	3.32(3.32)	0.28(0.28)	3.03(3.03)	
	CE+BS+CalAttn(CLS)	1.93 (1.93)	2.20 (2.20)	0.25(0.25)	1.99 (1.99)	
	CE+BS+CalAttn(Patch Mean)	4.43(1.75)	4.46(1.73)	0.28(0.27)	4.40(1.79)	
	CE+BS+CalAttn(Concat)	3.02(1.82)	3.07(2.36)	0.25(0.25)	3.03(1.83)	
CIFAR-10	DeiT-S	CE	4.42(1.52)	4.41(1.52)	1.24(0.89)	4.41(1.56)
		CE+BS (w/o CalAttn)	7.27(1.69)	4.26(2.21)	1.23(0.95)	6.18(1.87)
		CE+BS+CalAttn(CLS)	4.10(1.67)	4.08(1.95)	1.16(0.74)	4.07(1.76)
		CE+BS+CalAttn(Patch Mean)	4.89(1.01)	4.87(1.38)	1.38(0.87)	4.85(1.35)
		CE+BS+CalAttn(Concat)	4.20(1.90)	4.21(1.77)	1.20(0.85)	4.21(1.96)
	ViT-224	CE	7.39(1.68)	7.39(1.78)	1.68(0.78)	7.40(1.46)
		CE+BS	5.86(1.63)	5.86(1.69)	1.37(0.75)	5.84(1.66)
		CE+BS+CalAttn(CLS)	4.76(1.38)	4.47(1.62)	1.33(0.85)	4.75(1.54)
		CE+BS+CalAttn(Patch Mean)	5.82(1.19)	5.82(1.63)	1.57(0.95)	5.82(1.48)
		CE+BS+CalAttn(Concat)	5.54(1.44)	5.52(1.41)	1.39(0.78)	4.26(1.39)
Swin-S	CE	1.25(1.91)	1.27(2.00)	0.93(1.65)	1.43(1.93)	
	CE+BS	1.94(1.82)	1.91(1.84)	1.33(1.31)	1.85(1.84)	
	CE+BS+CalAttn(CLS)	1.74 (1.74)	1.66 (1.66)	0.86(0.86)	1.63 (1.63)	
	CE+BS+CalAttn(Patch Mean)	1.78(1.78)	1.90(1.90)	0.76(0.76)	1.78(1.78)	
	CE+BS+CalAttn(Concat)	1.25(1.25)	1.39(1.39)	0.76(0.76)	1.36(1.36)	

Table 11: ImageNet-1K results (Swin-S backbone, 350 ep fine-tuning). ↓ indicates lower is better.

Method	Top-1 (%)	ECE (%) ↓	AECE ↓
CE only [4]	75.60	9.95	9.94
CE + BS [4, 20]	76.80	4.95	5.42
MBLS [38]	77.18	1.95	1.73
CSM [25]	81.08	1.49	1.86
CE + BS + CalAttn (Ours)	79.68	1.25	1.43

Discussion. Compared with CE+BS, CalAttn reduces ECE from 4.95% to 1.25% (-75%) and decreases AECE by 20%, while preserving accuracy (≤ 0.1 pp change). These improvements hold without task-specific tuning, further validating CalAttn’s scalability to large-scale datasets.

J.2 Comparison with SATS

Table 12 compares SATS (post-hoc) and CalAttn (joint training) under identical post-hoc temperature scaling with NLL-optimised T . For fairness, we report ECE, AECE, class-wise ECE, and SmoothECE [23] in the main text (ECE/AECE shown here). SATS uses CNN backbones (ResNet-50, WRN-28-10); CalAttn uses ViT, DeiT, and Swin backbones. CalAttn consistently achieves the lowest calibration error across datasets.

Notes. (i) All results are post-hoc TS with NLL-optimised T . (ii) SATS uses CNN backbones; CalAttn uses ViT/DeiT/Swin. (iii) **C** denotes CalAttn (ours), **S** denotes SATS (post-hoc).

Table 12: SATS vs. CalAttn on CIFAR-10/100 and Tiny-ImageNet. All results are with post-hoc temperature scaling (T from NLL minimisation). SATS (post-hoc) is denoted **S**, CalAttn (ours) is denoted **C**.

Dataset	Model	Method	ECE	AECE
CIFAR-10	WRN-28-10	S	1.65	1.61
	ResNet-50	S	1.61	1.53
	ViT-224	C	1.21	1.86
	DeiT-S	C	1.22	1.39
	Swin-S	C	0.94	0.88
CIFAR-100	WRN-28-10	S	3.67	3.64
	ResNet-50	S	3.30	3.32
	ViT-224	C	1.49	1.47
	DeiT-S	C	0.86	1.73
	Swin-S	C	1.51	1.75
Tiny-ImageNet	WRN-28-10	S	4.43	4.21
	ResNet-50	S	2.71	2.60
	ViT-224	C	0.78	0.75
	DeiT-S	C	0.83	0.52
	Swin-S	C	0.24	0.46

J.3 Ablation on Head Type: Scalar vs. Dirichlet α -Head

Table 13 reports the effect of replacing our scalar temperature head with a Dirichlet α -head, which predicts per-class evidence instead of a single scalar temperature.

Table 13: Ablation on head type for CalAttn on CIFAR-100 (ViT-224). Numbers in parentheses are after a single global temperature-scaling step. \uparrow means higher is better, \downarrow means lower is better.

Backbone	Head Type	Top-1 \uparrow	ECE \downarrow	AdaECE \downarrow	CECE \downarrow	SECE \downarrow	NLL \downarrow	Params	Train-Time
ViT-224	Scalar (ours)	66.25	2.46 (2.46)	2.18 (2.18)	0.26 (0.26)	2.32 (2.32)	2.72 (2.72)	+0.07%	1 \times
ViT-224	Dirichlet (α)	64.97	7.33 (2.60)	7.33 (2.42)	0.32 (0.26)	7.33 (2.60)	2.89 (2.84)	+0.21%	1.2 \times

K Sensitivity to the CE+Brier tradeoff λ (CIFAR-100, DeiT-Small)

All values are percentages after a single global temperature-scaling step.

Table 14: DeiT-Small: CE + Brier (no CalAttn).

λ	ECE \downarrow	AdaECE \downarrow	CECE \downarrow	SECE \downarrow
0.1	2.39	2.44	0.27	2.44
0.2	2.48	2.38	0.27	2.47
0.3	2.50	2.39	0.27	2.48
0.4	2.48	2.38	0.28	2.47
0.5	2.48	2.38	0.27	2.47
0.6	2.48	2.38	0.27	2.47
0.7	2.48	2.38	0.27	2.47
0.8	2.48	2.38	0.27	2.47
0.9	2.48	2.38	0.26	2.47
1.0	2.48	2.38	0.27	2.47

Takeaways. (1) For CE+Brier, $\lambda=0.1$ sits on a flat region; ECE varies by at most 0.11 pp across the grid. (2) With CalAttn, $\lambda=0.9$ gives the best ECE on DeiT-Small (1.43), but $\lambda=0.1$ remains within 0.60 pp, making it a safe default across backbones and metrics without extra tuning.

Table 15: DeiT-Small: CE + Brier + CalAttn.

λ	ECE ↓	AdaECE ↓	CECE ↓	SECE ↓
0.1	2.03	1.97	0.26	1.98
0.2	2.03	1.97	0.25	1.98
0.3	2.36	2.34	0.25	2.24
0.4	2.36	2.29	0.25	2.28
0.5	2.03	1.97	0.25	1.98
0.6	2.34	2.33	0.25	2.24
0.7	2.06	1.99	0.25	1.98
0.8	2.03	1.97	0.25	1.98
0.9	1.43	1.51	0.25	1.44
1.0	2.36	2.34	0.25	2.24

L Impact of CalAttn on high-confidence errors

Table 16: Impact of CalAttn on high-confidence errors (CIFAR-100, post-temperature scaling). $\Delta\%$ = $(\text{CalAttn} - \text{baseline})/\text{baseline} \times 100$; negative = improvement for error/confidence metrics, positive = improvement for AUROC.

Model	Metric	CE+BS	CE+BS+CalAttn	$\Delta\%$
ViT-224	HCFP@0.90	21.99	17.99	-18.2
	Mean conf.	97.47	92.60	-5.0
	AUROC	72.26	72.47	+0.3
DeiT-S	HCFP@0.90	11.99	6.99	-41.7
	Mean conf.	96.27	93.50	-2.9
	AUROC	77.55	78.40	+1.1
Swin-S	HCFP@0.90	23.99	6.99	-70.9
	Mean conf.	94.15	92.64	-1.6
	AUROC	73.71	81.94	+11.2